

# STARS

University of Central Florida  
**STARS**

---


Electronic Theses and Dissertations, 2004-2019

---

2008

## Forensic Analysis Of Automobile Paints By Atomic And Molecular Spectroscopic Methods And Statistical Data Analyses

Erin McIntee  
*University of Central Florida*

 Part of the [Chemistry Commons](#), and the [Forensic Science and Technology Commons](#)  
Find similar works at: <https://stars.library.ucf.edu/etd>  
University of Central Florida Libraries <http://library.ucf.edu>

This Masters Thesis (Open Access) is brought to you for free and open access by STARS. It has been accepted for inclusion in Electronic Theses and Dissertations, 2004-2019 by an authorized administrator of STARS. For more information, please contact [STARS@ucf.edu](mailto:STARS@ucf.edu).

---

### STARS Citation

McIntee, Erin, "Forensic Analysis Of Automobile Paints By Atomic And Molecular Spectroscopic Methods And Statistical Data Analyses" (2008). *Electronic Theses and Dissertations, 2004-2019*. 3627.  
<https://stars.library.ucf.edu/etd/3627>



FORENSIC ANALYSIS OF AUTOMOBILE PAINTS BY ATOMIC AND  
MOLECULAR SPECTROSCOPIC METHODS AND STATISTICAL DATA  
ANALYSES

by

ERIN MAUREEN MCINTEE  
B.S. University of Florida, 2002

A thesis submitted in partial fulfillment of the requirements  
for the degree of Master of Science  
in the Department of Chemistry  
in the College of Sciences  
at the University of Central Florida  
Orlando, Florida

Fall Term  
2008

## ABSTRACT

The analysis of 110 automotive paint samples was conducted for the research presented here. Laser-induced breakdown spectroscopy (LIBS) was the central instrument utilized for analysis although scanning electron microscopy / energy dispersive x-ray spectroscopy (SEM/EDS) and Fourier transform infrared spectroscopy – attenuated total reflection (FTIR-ATR) analyses were also performed. Two separate methods of LIBS analysis of samples were used: a cross sectional analysis and a drill down analysis. SEM/EDS analysis focused on the cross section while FTIR-ATR analysis concentrated on the clearcoat layer. Several different data/statistical analyses were evaluated including principal components analysis (PCA), two tailed t-tests based on several different metrics (Hit Quality Index (HQI), Pearson's correlation and Sorenson index), multivariate analysis of variance and receiver operating characteristic (ROC) curves. Full spectrum data analysis from LIBS spectra resulted in 99.7% discrimination between different sample comparisons and 12% between same sample comparisons based on HQI and t-tests. Peak analysis of LIBS spectra resulted in 87.5% discrimination between different sample comparisons and 5% between same sample comparisons based on MANOVA. When combining the results of the FTIR-ATR and SEM/EDS analyses, 88% of the samples could be discriminated.

## ACKNOWLEDGMENTS

I would like to thank my mother, Kristine McIntee, and Nancy Rudner for urging me to go back to school; Dr. Candice Bridge for schooling me in LIBS and Excel; Dr. Liquiang Ni for exposing me to more statistics than I ever thought possible; Dr. Michael Sigman for being a super-advisor as well as heading my thesis committee; Drs. Barry Fookes and Andres Campiglia for also serving on my committee and reminding me of things I thought I had forgotten; Jessica Frisch for showing me the way and all the amusing drama; Emilie Viglino for being the best intern/"slave" ever; and Mary Williams for instruction with the SEM/EDS. I would also like to express thanks to Jeffrey Smith for his unwavering support as well as Lauren, Michael, Robert and Thomas McIntee for giving me well needed distraction and perspective.

“Sometimes I lie awake at night and ask ‘Why me?’ Then a voice answers ‘Nothing personal, your name just happened to come up.’” – Charles M. Schulz

“There are three kinds of lies: lies, damned lies, and statistics.” – Benjamin Disraeli

# TABLE OF CONTENTS

LIST OF TABLES .....	viii
LIST OF FIGURES .....	ix
CHAPTER 1: GENERAL INTRODUCTION .....	1
Automotive Paint .....	1
Components .....	1
Structure .....	6
OEM.....	7
Refinished .....	9
Previous Forensic Analysis.....	10
Instrumental Analyses.....	12
Laser-Induced Breakdown Spectroscopy .....	13
Theory .....	13
Previous work .....	15
Instrumental Setup .....	16
Fourier Transform Infrared Spectroscopy-Attenuated Total Reflectance (FTIR-ATR) .....	18
Scanning Electron Microscope / Energy Dispersive X-Ray Spectroscopy (SEM/EDS) .....	20
Theory .....	20
Instrument .....	21
Data Analysis .....	22
Pretreatment .....	23

Full Spectrum.....	25
Hit Quality Index .....	25
Principal Components Analysis.....	25
Correlation/Pearson.....	27
Sin <sup>2</sup> θ .....	27
Evaluation: Two-tailed t-test.....	27
Peak Analysis.....	29
Sorenson Index.....	29
Multivariate Analysis of Variance (MANOVA) .....	30
Receiver Operating Characteristics Curve.....	31
Distribution issues.....	32
Fisher’s Transformation.....	34
CHAPTER 2: EXPERIMENTAL.....	35
Samples.....	35
Instruments.....	35
Analysis.....	36
LIBS.....	36
Cross Section .....	37
Drill Down .....	38
FTIR-ATR.....	40
SEM/EDS.....	40
CHAPTER 3: LIBS Cross Section .....	42
Library.....	44

HQI and t-test.....	45
Reproducibility tests .....	46
Discussion.....	48
CHAPTER 4: LIBS DRILL DOWN .....	50
Substrate.....	53
Layer Identification.....	53
Library.....	54
Polyisobutylene Mounted Analyses.....	55
Full Spectrum.....	55
t-test.....	55
PCA/Cluster Analysis .....	57
Peak Analysis.....	65
Sorenson.....	65
MANOVA/ANOVA/Tukey.....	66
Discussion.....	71
CHAPTER 5: SEM/EDS & FTIR-ATR .....	76
SEM-EDS .....	76
Results.....	77
FTIR-ATR.....	77
Results.....	78
Discussion.....	81
CHAPTER 6: CONCLUSIONS AND FUTURE RESEARCH .....	83
Conclusions.....	83

Future Research .....	84
Automotive Paint .....	84
LIBS .....	84
Distribution free analysis .....	85
Combination Plots.....	87
APPENDIX.....	90
REFERENCES .....	96



## LIST OF TABLES

Table 1. Pigments used in automotive paint .....	4
Table 2. Summary of details of research experiments .....	36
Table 3. Results from the HQI/t-test cross section analysis .....	45
Table 4. Different sample discrimination of reproducibility experiments.....	47
Table 5. Same sample discrimination of reproducibility experiments .....	47
Table 6. T-test results based on HQI values from drill down spectra.....	56
Table 7. T-test results based on Z(r) values from drill down spectra .....	57
Table 8. Sorenson/t-test discrimination percentages based on drill down spectra .....	65
Table 9. Tukey discrimination matrix for Wavelength 1 (394.43 nm).....	68
Table 10. Overall discrimination of samples by MANOVA .....	70
Table 11. Wavelengths used for MANOVA, their possible elemental identification and discrimination .....	71
Table 12. Review of results from data analysis of drill down spectra.....	73
Table 13. T-test results from SEM/EDS analysis .....	77
Table 14. Results from the t-tests based on HQI from the FTIR-ATR spectra. ....	79
Table 15. Combination of results from SEM/EDS and FTIR-ATR analyses.....	80
Table 16. Percent discrimination of different comparisons outside of the confidence volume.....	88

## LIST OF FIGURES

Figure 1: Examples of monomers and binders .....	2
Figure 2. Paint chip structure for original equipment manufacture .....	7
Figure 3. LIBS setup .....	17
Figure 4. LIBS automotive paint spectrum.....	18
Figure 5. EDS spectrum of cross section of Pontiac GTO .....	21
Figure 6. Original (top) and baseline corrected (bottom) spectra.....	24
Figure 7. Two analysis methods .....	37
Figure 8: Cross Section Analysis (paint chip not drawn to scale) .....	38
Figure 9. Spectra of polyisobutylene at different thicknesses .....	39
Figure 10. Drill Down Analysis.....	39
Figure 11. Stereomicrograph (50.4X) of sample preparation for SEM/EDS analysis.....	41
Figure 12. Normalized spectra from three samples from the cross section analysis .....	43
Figure 13. ROC analysis of replicate cross section analyses.....	44
Figure 14. Distribution of same sample comparison and different sample comparison for t-test.....	46
Figure 15. Micrograph of laser ablation of burn paper at decreasing laser energy levels	50
Figure 16. Micrograph of the crater formed from a single laser pulse on a paint sample	51
Figure 17. Averaged drill down spectra of 1987 Dodge Ram (a) and 2005 Mazda Tribute (b).....	52
Figure 18. Contour surface plots based on Pearson correlation values comparing spectra within the same drill down.....	54
Figure 19. ROC analysis of Library analysis of drill down spectra.....	55

Figure 20. Scree plot of eigenvalues from PCA of non-baseline corrected spectra .....	58
Figure 21. Cluster analysis dendograms based on principal components (3: top; 7: bottom) based on NBC spectra .....	59
Figure 22. Principal components plot based on PCA of NBC spectra .....	60
Figure 23. Scree plot of eigenvalues based on PCA of NBC spectra normalized by the 2 <sup>nd</sup> method.....	61
Figure 24. Cluster analysis dendogram of 3 principal components based on NBC spectra .....	62
Figure 25. Plot of three principal components obtained from PCA of NBC spectra.....	63
Figure 26. Cluster analysis dendograms of principal components (4: top; 5: bottom) based on BC spectra.....	64
Figure 27. Representative averaged spectra from PCA/cluster data analysis.....	74
Figure 28. EDS spectrum of Pontiac GTO .....	76
Figure 29. FTIR-ATR transmittance spectrum of the clearcoat of 2005 Pontiac GTO...	78
Figure 30. Combination plots using three calculated values .....	87

# CHAPTER 1: GENERAL INTRODUCTION

Automobile paint has been found at crime scenes such as hit-and-runs as well as other automobile accidents in numerous cases over the last 75 years. Several articles have documented the probative value of automotive paint,<sup>1-3</sup> and different approaches to its analysis have been developed and standardized over the years.<sup>4</sup> This research focuses on automobile paint analysis with the primary utilization of laser-induced breakdown spectroscopy (LIBS). Fourier transform infrared spectroscopy (FTIR) and scanning electron microscopy / energy dispersive x-ray spectroscopy (SEM/EDS) are also explored and incorporated into the data analysis which covers a variety of approaches in its pursuit of discriminating between paint samples.

## Automotive Paint

Automotive paint is classified as a surface coating. It serves dual purposes as both a decorative and a functional coating. It serves as a way to create something pleasing to the eye by “hiding” the lower substrate. It also protects the metal or plastic body from degradation due to environmental elements such as ultraviolet rays, salt, and oxygen; and from injury due to contact with rocks and other cars.<sup>5</sup>

## Components

Paint in its unapplied form consists of three main components: binder, pigment and solvent. Additives are also developing into an increasingly important part in paint formulations. In a single paint sample, each component can be made up of many different compounds. Each compound contributes its own part to the underlying purposes of protection and decoration.

The majority of solids within the paint consist of the binder also called the resin. The binder is responsible for adhesion and cohesion: ensuring that the paint remains attached to the substrate while keeping the pigment within the coating. In the past, these typically consisted of high weight polymers which required a large amount of solvent to dissolve and apply. The large amount of solvent also resulted in very thin layers, which required multiple applications in order to gain the required thickness. However, the use of lower weight monomers that, after evaporation of the solvent, crosslink forming larger weight polymers has increasingly become more popular. The polymers are usually synthetic and examples of these include epoxies, polyesters, alkyds (oil-included polyester), melamine and acrylics, shown in Figure 1 below.

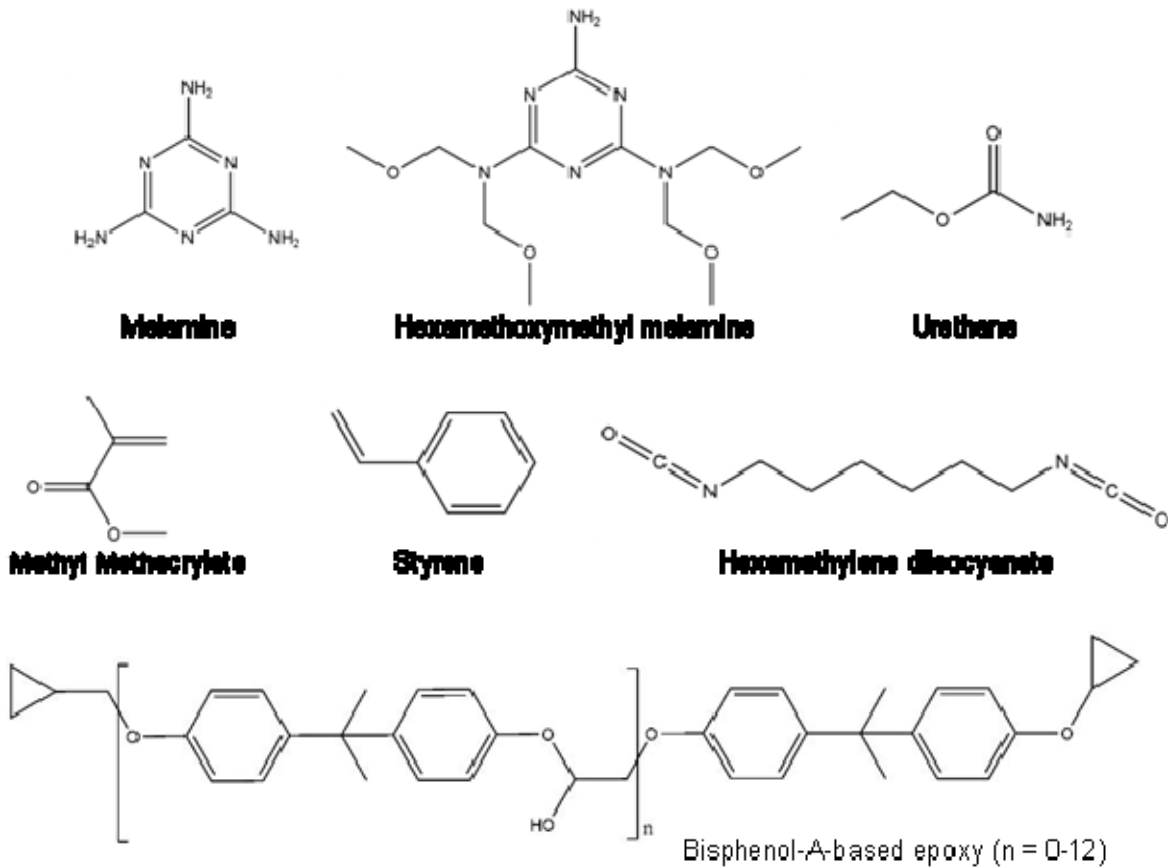
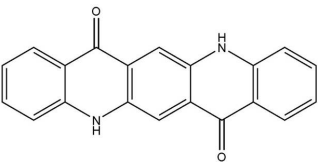
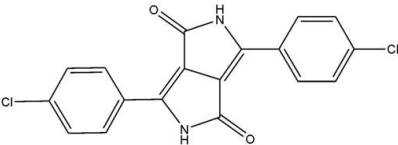
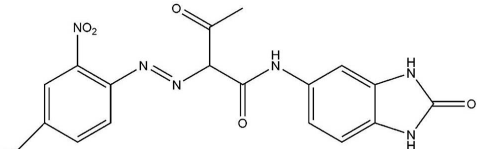
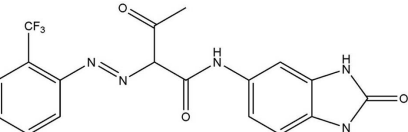
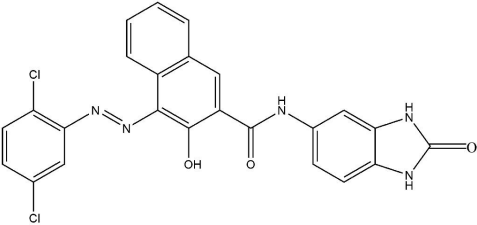
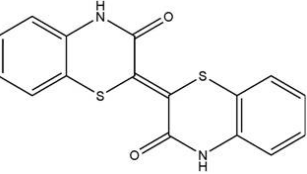
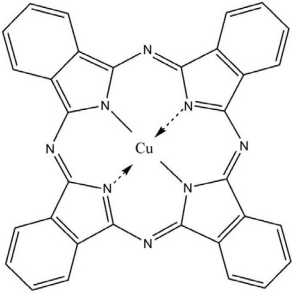
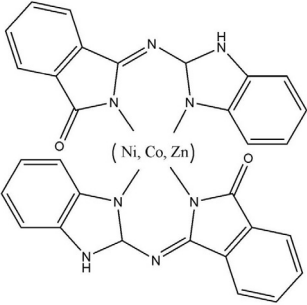


Figure 1: Examples of monomers and binders

As was mentioned previously, mixtures of different monomers, such as formaldehyde with melamine, urea or phenol, are combined to obtain the desired durability and flexibility. The compounds crosslink upon stoving, which is heating at a high temperature (~165°C), and provide a strong, durable coating. Isocyanates are also used to crosslink the resin. These are often blocked for application with groups such as alcohols or lactams of low molecular weight.<sup>5</sup> Upon heating, the reversible covalent bond between the blocking group and the isocyanate is broken and the blocking groups are lost through evaporation to allow for crosslinking. The traditional binders have given way to “high solids, solvent free, powder, waterborne and non-aqueous dispersion media.”<sup>6</sup>

The pigment primarily provides color and opacity. It can also impart other protective properties such as UV protection, glossiness and durability. Pigments can be organic or inorganic, natural or synthetic. The principle black and white pigments are inorganic, carbon black and titanium dioxide (TiO<sub>2</sub>) respectively, while colored pigments are typically organic because they tend to give truer, brighter colors. Table 1 displays examples of pigments used in automotive finishes. In some cases pigments contain both organic and inorganic components, as in the phthalocyanine pigments, which consist of an inorganic element (e.g. Cu<sup>2+</sup>) coordinated with the nitrogen atoms on the organic structure (Table 1). In the pigmented basecoat, more than one pigment may be used to produce the desired color especially with organic pigments, for example a quinocridone with a diketopyrrolopyrrole (PR 254).

Table 1. Pigments used in automotive paint

Inorganic Pigments		
White Titanium dioxide – TiO <sub>2</sub>	Color Bismuth Vanadate – BiVO <sub>3</sub> Cerium Sulfide – Ce <sub>2</sub> S <sub>3</sub> Yellow 53 – NiSbTi Brown 24 – CrSbTi Lithopone – ZnS/BaSO <sub>4</sub> Aluminum flakes Mica – KAl <sub>2</sub> (AlSi <sub>3</sub> O <sub>10</sub> )(F,OH) <sub>2</sub>	Black Carbon Black
Organic Pigments		
Quinocridone	Pigment 254	
		
PO 36	PY 154	
		
P. Br. 25	Thiazine	
		
Organic+Inorganic Pigments		
Copper Phthalocyanine Blue	PY 179	
		

Effect pigments have become significant in the paint industry. In 2000 it was estimated that ~70% of topcoats contained some form of effect pigment<sup>7</sup> and with the popularity of “tricking out” cars that number has understandably grown larger. These flakes or platelets reflect light differently based on the observation angle. Pigments giving special optical effects, referred to as a lightness or color “flop”, to the paint use a variety of substrates and coatings including coated mica platelets, silicate ( $\text{SiO}_2$ ) or alumina ( $\text{Al}_2\text{O}_3$ ) flakes.<sup>8</sup> Mica by itself gives a dull glimmer effect and is typically coated. It can be coated with a wide variety of materials (e.g.  $\text{TiO}_2$ ,  $\text{Fe}_2\text{O}_3$  and  $\text{SiO}_2$ ) separately and in combination. By varying the thickness of a coating on a mica platelet, the reflected color is also varied. As the paint dries, the pigments align parallel to the surface giving the effect.

With the exception of powder coatings, the solid binder and pigment need a vehicle in which they can be applied to a surface. Solvents dissolve or dilute the pigment and binder depending on the liquid, thereby aiding in the manufacture and application of the paint. The solvent evaporates with or without the aid of heat leaving behind the binder and pigment after the paint has been applied. Often solvents are organic compounds that are very toxic to humans and/or the environment. Increasingly, these organic solvents are being limited, replaced with waterborne and emulsion coatings or eliminated altogether in the case of powder coatings.

Other additives, which are also referred to as extenders, are included within the paint for a number of different reasons. Originally they were included to produce a less expensive product; however, the applications have expanded to include affecting drying, glossiness and interfacial and surface tension, guarding against micro-organisms and



aiding in applying paint to the surface.<sup>5,9</sup> With the introduction of waterborne paints, the need for additives has increased. Defoamers and wetters for the substrate and the clear coat are necessary ingredients for waterborne applications. With the increase in the use of organic pigments which are not as lightfast (tendency to fade) as inorganic pigments, UV stabilizers or blockers can be found specifically in the clearcoat.

There are situations in which the inclusion of three main components can be changed and even omitted. Powder coatings only contain a pigment and a binder. The paint is sprayed onto a surface or the substrate is dipped into the paint, and then baked to melt the components and create a coating on the surface. This method avoids using a costly and possibly hazardous solvent and does not necessitate the expensive equipment needed to dispose of the solvent. However, only certain binders and pigments are suitable for this type of application and layers can become too thick for car paint applications.

Paints can be applied in a number of different methods. Based on the substrate and paint's composition, the paint may be sprayed, dipped (electrodeposition), rolled, brushed, etc. The most common forms of application in the automotive industry are spraying and dipping. Spraying involves high rotational bells that depend on mainly centrifugal forces with slight electrostatic assistance for application of the paint. Dipping in the form of cathodic electrodeposition utilizes a positively charged substrate (metal) to attract solubilized epoxy or acrylic binders.<sup>10</sup> Layers upon stoving are even and thin.

### Structure

In the automotive industry, the responsibility of protection and decoration has been divided between layers of paint.<sup>10</sup> As such, automotive paint as trace evidence

usually presents itself as layered chips. These samples can be classified into two types: original equipment manufacture (OEM) and refinished.

## OEM

Chips with OEM paint have three to four layers consisting usually of a primer, surfacer, basecoat and clearcoat (Figure 2). The purpose of each layer is to protect the substrate and the layers below it, either through anticorrosive pigments or the physical thickness of the layer. The top two layers are responsible for decoration by imparting color and gloss.

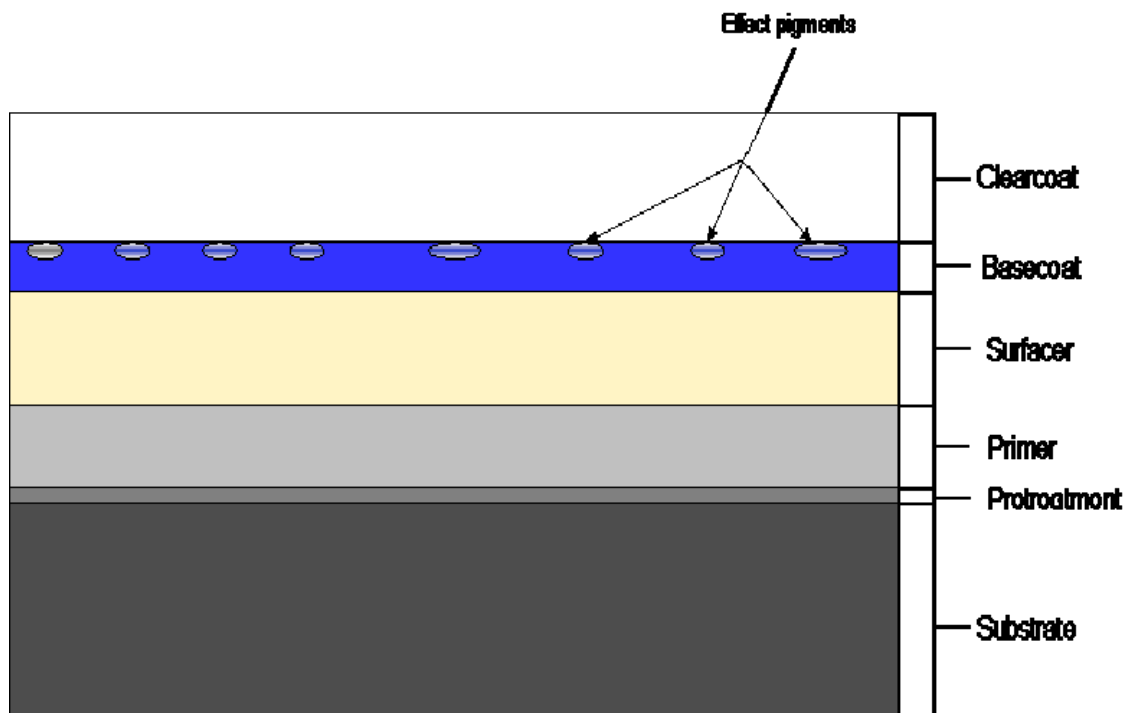


Figure 2. Paint chip structure for original equipment manufacture

The substrate (either galvanized steel or plastic) is cleaned and pretreated to form a phosphate conversion layer which is about one micrometer thick. This layer helps to

protect the substrate from corrosion and provides a platform for better adhesion of the successive paint layers.<sup>5, 7, 10, 11</sup> Then an electrocoat primer is applied to the surface. The primer usually consists of zinc phosphate in a waterborne epoxy resin that serves to protect the metal body from rust. The substrate is dipped in a bath, and through cathodic electrodeposition a 20-30  $\mu\text{m}$  layer is created.

An opaque surfacer is applied after the primer to hide the substrate and primer and sanded to provide a smooth surface for the next layer. It also provides protection from stone chipping of the primer. Binders used in this layer include polyesters which necessitate an organic solvent and polyester-melamine which can be used with waterborne systems. These layers are applied using an electrostatic spray and typically range between 30 and 40  $\mu\text{m}$ . Pigments in these types of layers are responsible for hiding the substrate, so they need to have a refractive index greater than that of the binder. Typically titanium dioxide is employed in this capacity.

The pigment-containing basecoat is subsequently applied, and often metal flakes or platelets, most often coated with rutile  $\text{TiO}_2$ , can be found in the colored basecoat. Two coats are usually applied, the first with an electrostatic spray then a second with compressed air. The second application contains the metal flakes and the compressed air helps to orient them parallel to the outer surface which allows for a total thickness of 15  $\mu\text{m}$  for this layer. The binders used in this layer are usually an acrylic or alkyd with melamine-formaldehyde crosslinking resin. The panel is kept warm for 3-5 minutes at 40-60°C.

The final addition of the clearcoat completes the painting process. This last layer protects the previous layers beneath it from mechanical as well as other types of damage

while also allowing the color from the pigments in the lower layer to be visible. For this reason, no pigments are found in the clearcoat which is usually about 40  $\mu\text{m}$  thick. The binders found in these layers are often acrylic melamine-formaldehyde systems with blocked isocyanates that crosslink upon stoving. The clearcoat also contains additives that protect pigments in the underlying layer from UV degradation. The basecoat and clearcoat are cured together as the last part of the application process.

### Refinished

A refinished automotive paint chip differs from an original manufacturer's paint chip in several ways. In most refinished samples, the number of layers exceeds four by means of painting over the OEM coatings; layers of up to 20 have been documented.<sup>12</sup> Since refinishers are not able to cure the paint at factory temperatures, solvents must be able to evaporate at ambient temperatures or at temperatures much lower than curing temperatures. For this reason, refinished layers can be characterized by the use of older, more traditional binders such as nitrocellulose that require the use of volatile organic compounds (VOCs).<sup>5</sup> The crosslinking found in OEM layers is absent in refinish samples. The presence of dust particles that would not exist in an OEM chip is also a differentiating factor. Since the method of application is often controlled by a person rather than a machine, the width of layers is also often greater than OEM and less consistent.

Since its beginnings, the automotive paint industry has been in a constant process of change. The reasons for this are often linked, for example the development of new products and introduction of new laws.<sup>11</sup> Specific elements and classes of compounds have been eliminated which have caused a gap in the market that has needed to be filled.

For example, thirty years ago lead was banned for use in paints because of its toxicity which required the industry to generate different sources for pigments. The bright colors produced by lead pigments were replaced by organic pigments. Another ingredient being influenced by legislation is chromium, which had been used as a pigment in the electrocoat and the basecoat. As mentioned above, chromium has been replaced by zinc phosphate in order to protect the substrate from corrosion in the electrocoat and other pigments in the basecoat.

A push towards a decrease in the consumption of VOCs, in particular polyaromatic hydrocarbons (PAHs), has been the most recent target in legislation.<sup>7</sup> Since they are derived from petroleum products and are essentially lost to the atmosphere after application, VOCs cost the paint industry in terms of disposal and raw products. For these reasons, high solids (decrease in VOC content), powder, and waterborne-based applications of paints have been developed which also affect the industry. The industry is also constantly looking for new and less expensive ways to produce and apply automobile paint.

#### Previous Forensic Analysis

Combining all of the factors mentioned in the previous section (paint components: binders + pigments+ additives; and at least four different layers) creates a very complex matrix. The layers themselves are also very thin which complicates analysis. While the automotive industry has provided crime labs with catalogues of paint samples, there is no standard sample for paint in order to compare results as is done with other regulated products, so only qualitative and semi-quantitative methods have been developed. These factors serve to obscure the analysis of paint.

Car paint analysis has primarily been carried out by visual observation as a first step, usually with a polarized light microscope or stereomicroscope.<sup>13</sup> By examining a paint cross section, the number and thickness of the layers and description of the layers can be determined; microscopy provides a quick and easy way of examining a sample. From there a microspectrophotometer is used to determine the color of the pigments found in each layer. The resulting spectrum as well as Commission International de l'Éclairage (CIE) color coordinates from the microspectrophotometer analysis is valuable in discriminating between samples.

The analysis usually then diverges between analyses of the organic and inorganic components. For analysis of the clearcoat, pigments and binders, the use of Fourier transform infrared spectroscopy<sup>14-16</sup> has extensively been documented by Suzuki, et al, among others.<sup>17, 18</sup> While creating a cross section with use of a microtome and collecting a transmission spectrum gives more reproducible results, obtaining a reflective spectrum is easier and less destructive.<sup>18</sup> An attempt at mapping layers using FTIR has been performed by Flynn, et al.<sup>17</sup> The Royal Canadian Mounted Police (RCMP) has developed the Paint Data Query (PDQ) Database that can search, compare and find similar FTIR spectra.

While FTIR has been valuable for forensic paint analysis, other instruments have also been evaluated. Pyrolysis gas chromatography mass spectrometry has also had some limited use.<sup>19</sup> It has proven to be slightly more successful in discriminating between samples<sup>20</sup> and the use of a laser for micro-pyrolysis appears to provide acceptable results<sup>21</sup>; however, it is destructive and sample preparation is time consuming. Similar to Py-GC/MS, Stachura et al, have explored laser desorption mass spectrometry that uses a

time-of-flight mass spectrometer to analyze pigments.<sup>22</sup> These types of analyses only identify the organic components of a paint chip.

For analysis of the inorganic components, scanning electron microscopy/energy dispersive X-ray spectroscopy<sup>23</sup> and laser ablation inductively coupled plasma mass spectrometry<sup>24, 25</sup> are the most widely-used techniques. SEM/EDS requires extensive sample preparation due to the nonconducting nature of a paint sample but has been able to discriminate between similarly colored car paints. Raman spectroscopy<sup>15</sup> has also been building in popularity for the identification of extenders and inorganic pigments, including effect pigments. X-ray diffraction (XRD)<sup>26, 27</sup> and X-ray fluorescence (XRF)<sup>28</sup> have also been developed as techniques to analyze the inorganic elements in paint samples. However, these techniques do not have a limit of detection as low as SEM/EDS analysis.

The benefit of using two of the previously mentioned analyses, such as FTIR with Raman or SEM/EDS, has been suggested in order to identify both organic and inorganic ingredients resulting in increased discrimination.<sup>29, 30</sup> While this is possible, it is not as probable since forensic scientists are limited in the amount of sample that is available to them. Other methods should be developed that are able to analyze both inorganic and organic components simultaneously.

### Instrumental Analyses

Three instruments were used in this research to analyze the automotive paint samples: laser-induced breakdown spectroscopy (LIBS) and Fourier transform infrared spectroscopy (FTIR) and scanning electron microscopy / energy dispersive X-ray spectroscopy. While FTIR and SEM/EDS are established methods of forensic paint

analysis as mentioned above, LIBS is a more recent technique and is the focus of the research here.

### Laser-Induced Breakdown Spectroscopy

LIBS offers contrasts to the previously mentioned instrumentation: little sample preparation, quick sample analysis and inexpensive instrumentation. Since the first observation of laser induced plasma in the 1960s, the field developed relatively slowly at first; however, with the development of more interest and improved detectors LIBS has progressed more rapidly in the past 15 years.

#### Theory

Lee, et al, has defined LIBS as an “elemental analysis based on the atomic emission from the plasma generated by focusing a powerful laser beam on a sample (solid, liquid or gas).”<sup>31</sup> The main difference between it and other plasma emission spectroscopy is that the plasma forms over the sample allowing for a simpler instrumental setup and a more convenient analysis than conventional atomic emission spectroscopy.

As the name infers, a laser is used to break down a sample and create the plasma. Different types of lasers can be employed in this type of instrument but commonly solid state pulsed lasers such as a neodymium: yttrium aluminum garnet (Nd:YAG) are found in many instruments. Ruby, gas and excimer lasers have also found use in LIBS instruments. The lasers are pulsed for 5-10 nanoseconds; although, femtosecond lasers have also been explored as possibly more beneficial for analysis.<sup>32</sup>

When energy from the laser pulse exceeds a critical threshold value, which is dependant on the sample, the sample rapidly heats, melts and becomes vaporized to



create a plasma which expands directly above the sample toward the focusing lens. In order for the plasma to form, free electrons must be generated, and an avalanche ionization must occur.<sup>33</sup> A plasma is “a local assembly of atoms, ions and free electrons, overall electrically neutral, in which the charged species often act collectively.”<sup>34</sup> The ratio of the different species changes throughout the lifetime of the plasma which lasts only a few hundred microseconds. The temperature within the plasma can reach tens of thousands of degrees (Kelvin).

During the first ~100 ns, a high white light continuum and a shock wave can be observed. The continuum results from a combination of bremsstrahlung and recombination events within the plasma. After this period, discrete lines from the elements in the plasma can be observed. To reduce the continuum interference, time-resolved spectra are taken by delaying the gate of the spectrometer.

Detectors are divided into two categories: 1) photodiodes and photomultipliers and 2) photodiode arrays, charged coupled devices (CCDs) and charge-injection devices. The second type was used in this research, specifically charged coupled devices. Several of this type of detector can be used to encompass a broad range of wavelengths. This allows a wider variety of elements to be detected with the same instrument.

Although it was mentioned previously that LIBS is an atomic analysis, diatomic species can also be observed in the spectra, specifically C<sub>2</sub> and CN bands. These bonds originate from recombinations of two atoms from the sample or one atom from the sample and one from the atmosphere (nitrogen).<sup>35</sup>



## Previous work

Laser induced breakdown spectroscopy has been explored for numerous applications. Because of its minimal sample destruction, quick analysis time and limited sample preparation, several areas have explored its use. For example, the historical preservation and yet scientific need to explore the contents of certain valuable objects (i.e. historical documents and paintings, etc.) has propelled the research to explore the use of LIBS. LIBS has been used to determine the best laser cleaning process when preserving historical paper documents.<sup>36</sup> It has also been used to characterize cinematographic films for conservation purposes.<sup>37</sup> LIBS has been used to distinguish between layers in ceramics as well as other layered samples.<sup>38</sup> Tool steel and glass have been analyzed using microscopic LIBS in which a microscope objective is used to focus the light from the laser to a one micrometer focal spot.

The data analysis of LIBS spectra has been approached in several ways. These include correlation analysis, a calibration-free method and others. Lentjes has advocated the use of correlation methods, and Gornushkin et al has demonstrated its advantages over the rank (Spearman) correlation.<sup>39</sup> Principal components analysis (PCA) has been employed in use of grouping soil data using LIBS.<sup>40</sup>

Forensic science has also deemed LIBS a potential method of analyzing evidence. LIBS has been used to investigate the analysis of solid, liquid and gas samples and to discriminate between matrices such as glass.<sup>41,42</sup> Residue explosives analysis has also used LIBS as a stand-off method of detection.<sup>43,44</sup> It has also been used to map latent fingerprints<sup>45</sup> and analyze gunshot residue.<sup>46</sup> The analyses of human remains and prosthetic implants have also been conducted using LIBS providing a forensic use.<sup>47</sup>

Some problems encountered using LIBS include matrix effects, self-absorption, line broadening and background radiation. Borisov, et al, explored fractionation and signal intensity as a function of crater development (for LA-ICP-MS).<sup>48</sup> Fractionation, which is the tendency of certain analytes to be sampled preferentially to other analytes, was also the subject of an article by Outridge that explored the relationship between the melting point and non-representative sampling of a glass sample.<sup>49</sup> These problems can be limited but not entirely eliminated. In order to limit some of these effects, Čtvrtníčková, et al, have experimented with limiting the amount of light to the center of the plasma in order to obtain better spectra.<sup>50</sup> Castle, et al, also inputs several variables for reproducibility in LIBS when analyzing copper.

### Instrumental Setup

A commercial LIBS instrument (model LIBS2000+) from Ocean Optics (Dunedin, FL, USA) was used during the research. The setup for the LIBS instrumentation can be seen in Figure 3. The neodymium: yttrium aluminum garnet (Nd:YAG) pulsed laser (Big Sky Lasers, model CFR200, Bozeman, Montana, USA) emits at the fundamental wavelength of 1064 nm for a pulse width of 9 ns. The laser is focused through a single lens ( $f = 7.5$  cm) onto the sample. The sample is located within a chamber on a movable stage that can be shifted in both X and Y directions.

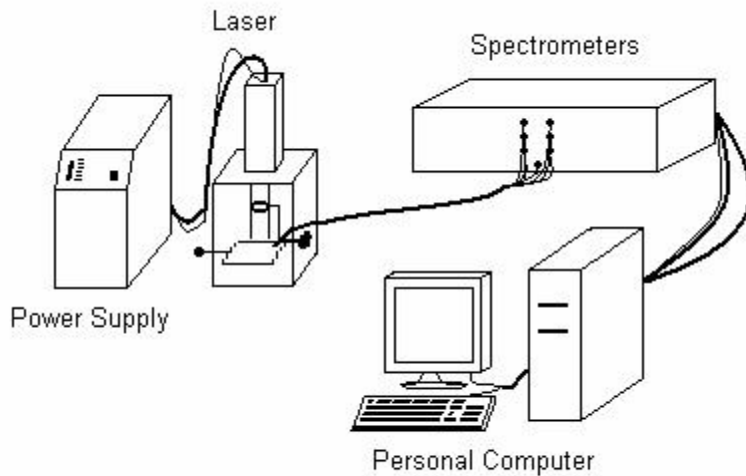


Figure 3. LIBS setup

The emitted light from the plasma is then collected by a bifurcated set of optical fibers, oriented  $45^\circ$  to the incident laser beam. The fibers connect to a train of seven separate linear CCD array spectrometers which detect from 198.14 to 965.43 nm. The spectrometers have a range of resolutions from 0.04-0.07 nm. A personal computer equipped with Ocean Optics OOILIBS software then acquires the data detected by the spectrometers. The software also controls the firing of the laser by controlling the Q-switch within the laser. A typical LIBS spectrum from a paint sample can be seen in Figure 4. The software allows for a spectrum from either a single plasma event to be recorded or the average of a specified number of pulses.

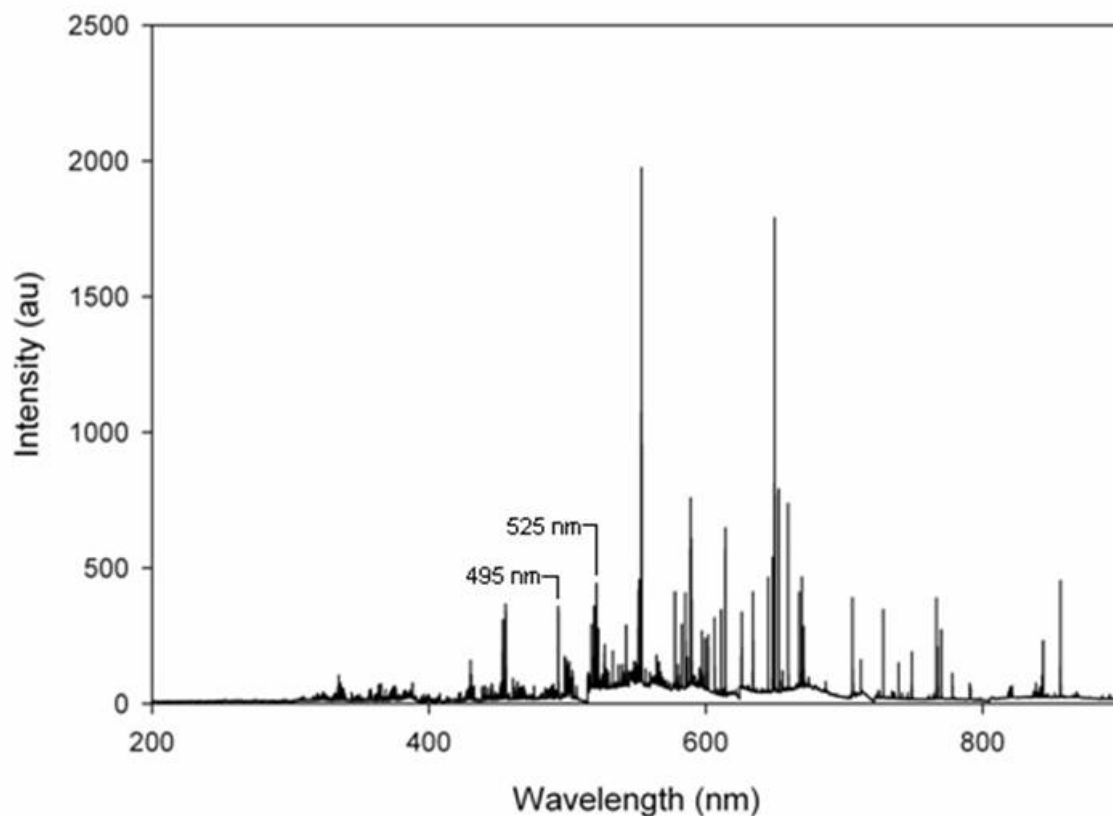


Figure 4. LIBS automotive paint spectrum

#### Fourier Transform Infrared Spectroscopy-Attenuated Total Reflectance (FTIR-ATR)

Infrared spectroscopy is based on the transitions of molecules from one vibrational level to another.<sup>51</sup> In order for vibrations to be IR active, they must be associated with changes in the permanent dipole. Spectra are collected in the mid-infrared, approximately  $4000\text{-}400\text{ cm}^{-1}$ . The spectra indicate the vibrations (symmetrical and asymmetrical stretching, scissoring, wagging, twisting and rocking) that a molecule exhibits when exposed to infrared light. Samples can be liquid, solid or gas.

The FTIR-ATR instrument consists of a silicon-carbide source which emits broadband radiation in the mid-infrared wavelength range. The radiation from the source passes to the Michelson interferometer. Within the interferometer, the radiation is directed to one of two mirrors, one which is stationary and another which oscillates continually between two distances. The radiation is reflected back by both mirrors and recombines creating an interference pattern which can be constructive or destructive depending on the position of the movable mirror. A HeNe laser (632 nm) with a high frequency also passes through the interferometer so that the resolution can be established.

The optics of the attached microscope focus the radiation from the interferometer to the sample, which has been previously brought into focus. The sample reflects or transmits the light to the mercury cadmium telluride (MCT) detector. The signal from the detector is converted mathematically from the time domain to a frequency domain with the use of a Fourier transform. Several spectra are usually averaged in order to obtain a spectrum with relatively little noise.

The attenuated total reflectance attachment allows for analysis of samples where the radiation is passed through a silicon crystal of high refractive index relative to the sample such that an evanescent wave is created. The sample absorbs the radiation at certain wavelengths and reflects back the attenuated energy from the evanescent wave.<sup>52</sup> This can be done with solids such as films, pastes and powders. The ratio between the peaks in the spectra using the ATR attachment are not the same as with a transmission spectrum but generally the same peaks are observed allowing for determination of the compound.<sup>53</sup>

## Scanning Electron Microscope / Energy Dispersive X-Ray Spectroscopy (SEM/EDS)

### Theory

The SEM/EDS energizes a sample by directing a beam of electrons to the sample.<sup>54</sup> The products of interest in the interactions between the electron beam and the sample are of three kinds: backscatter (BS) electrons, secondary (S) electrons and X-rays. Backscatter electrons are inelastic scattering of electrons from the beam after interaction with the sample with minimal loss of kinetic energy. They can provide qualitative information about a sample as well as imaging capabilities. Secondary electrons are the next most probable event in this situation; the electron beam stimulates the sample to release an electron that is loosely bound. Backscatter and secondary electrons are important for imaging and qualitative analysis of the sample.

Finally, the third, most infrequent and important to quantitative analysis, are the X-rays produced by the interaction of the electron beam with the sample. The electrons from the beam excite an electron in the inner three shells of the atom within the sample (K, L and M). Because of this energy, the electron is ejected from the atom. The atom is left in an excited state, and as the atom comes back to the ground state it gives off X-rays indicative of the energy. The X-rays intensities are generally reported as energies and are plotted as a spectrum (Figure 5).

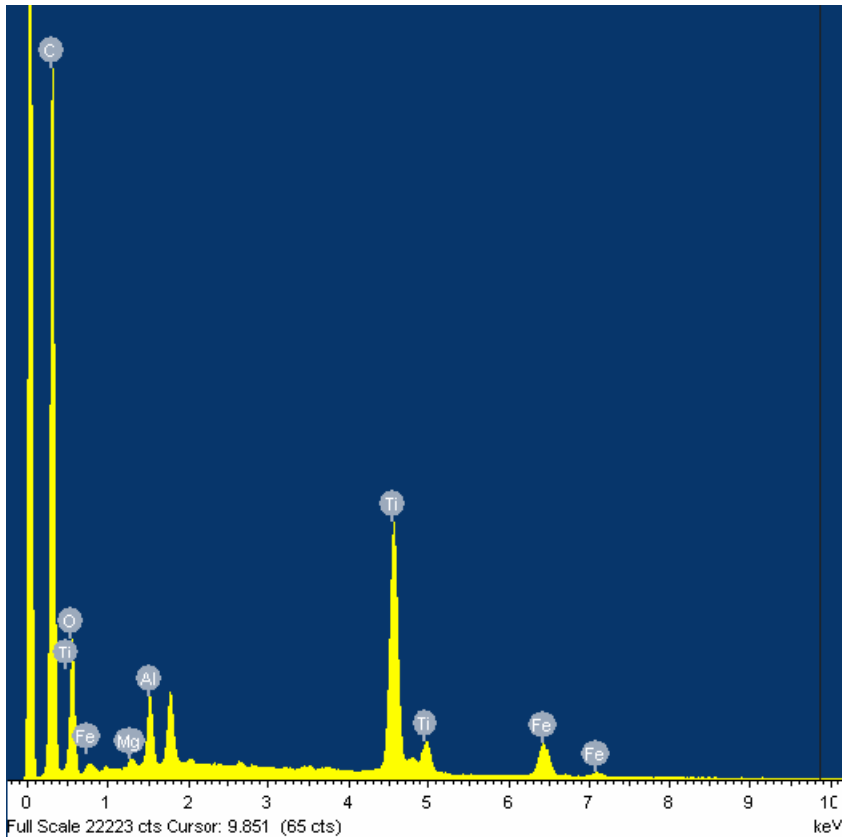


Figure 5. EDS spectrum of cross section of Pontiac GTO

## Instrument

The source of the electron beam is most commonly a tungsten filament although lanthanum hexaboride ( $\text{LaB}_6$ ) filaments can also be utilized.<sup>54</sup> A high negative voltage is maintained through the filament which is shaped like a hairpin. Due to the heat produced by the voltage, electrons from the filament are emitted and travel toward the anode (ground potential) and through a set of electromagnetic lenses which, similar to their optical counterparts, serve to collimate and focus the beam. The beam is rastered across the area of the sample to be analyzed with the use of scan coils creating an image from the BS and S electrons and X-rays for detection by the EDS.



The X-rays are collected at a specific angle to the sample and are detected through the use of a lithium-drifted silicon (Si(Li)) crystal. The crystal produces photoelectrons which are detected and amplified. Since the X-ray events are rare it is important to eliminate as much instrument noise as possible. For this reason, the Si(Li) crystal and detector needs to be cooled through the use of liquid nitrogen. A computer controls and displays all images and data from the detectors.

Although detection of lighter elements down to beryllium is possible with a windowless EDS, the resolution between the different x-rays from elements found below 1 keV becomes poor.<sup>54</sup>

### Data Analysis

Several different approaches were explored to analyze the data collected from all experiments. The first few are based on common comparisons used by multiple computer software packages while others are based on work by previous LIBS researchers as detailed above. Previous research on glass<sup>41</sup> laid the groundwork for this data analysis. However glass and paint spectra are very different visually.

The data analysis has been divided into two different sections based on what is being analyzed: the full spectrum or specific peaks. The focus of the data analysis discussed here was on devising a method to use the entire spectrum since it would seem to be more advantageous to use all possible information gathered during the experiment. The focus of the second section is a much more tedious process to individually select relevant peaks for analysis.

## Pretreatment

Due to the nature of spectral data, it is sometimes necessary to pre-treat the data in order to compare them. One process is normalization which scales the intensities in the spectra so that all spectra are on the same scale (e.g. have the same maximum intensity). This is necessary for some comparison procedures while not necessary for others. The general procedure used in this research was normalizing the spectra to unit vector length unless otherwise noted.

When comparing peaks, the most important factor is the intensity of the peaks. The baseline is indirectly linked to this calculation in that it partially determines the peak height. Each spectrometer used in the research has its own baseline which is slightly different from each other. For example in Figure 4, the peak at ~525 nm appears to have a greater intensity than the peak at ~495 nm due to the baseline shift in the fourth spectrometer. If the spectrum was baseline corrected, the peak at 525 nm would be less intense than the one at 495 nm.

However, this effect is reduced by baseline correcting the spectra; the true peaks and elimination of the false peaks - those that have high counts due to a high baseline, are obtained (see Figure 6). Baseline correcting the spectra can be as simple as subtracting a certain amount  $Y$  from each intensity to as complicated as iteratively fitting all points to a line. The baseline correction method used in this research uses the latter approach and was based on a method used by Coombes, et al. The method first locates the peaks and their bases, removes the peaks, and takes as the baseline the local minimum within a specified width. This baseline is subtracted from the original spectrum and the process is repeated a second time which then becomes the baseline corrected spectrum (Figure 6).<sup>55</sup>

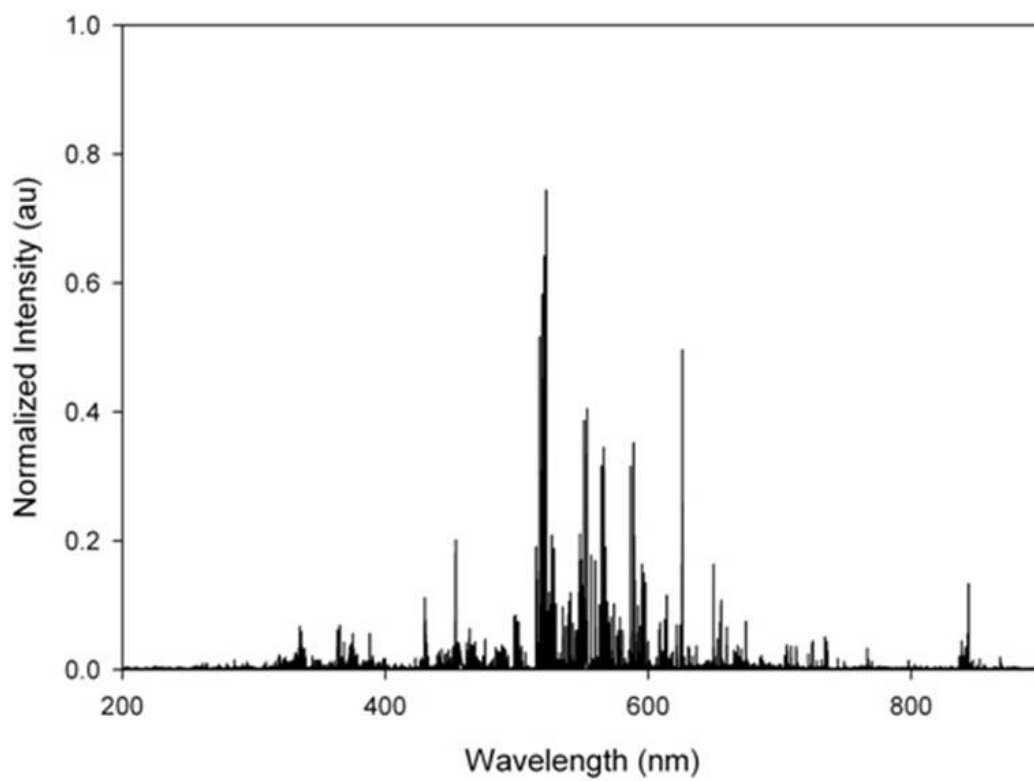
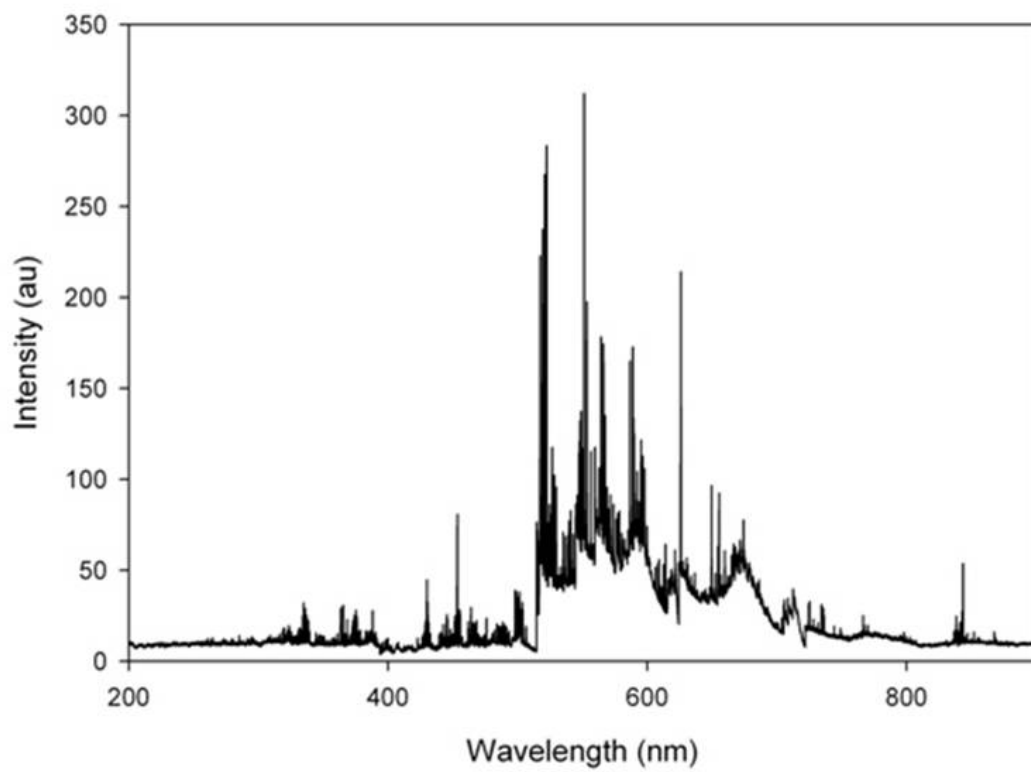


Figure 6. Original (top) and baseline corrected (bottom) spectra.

## Full Spectrum

In this research, the number of wavelengths that were monitored in a full LIBS spectrum was 13,696. Both normalized and baseline corrected spectra were used during these types of analyses.

## Hit Quality Index

The Hit Quality Index (HQI) is similar to a Euclidean measure of the distance between two spectra; HQI is based on the dot product between the spectra.<sup>56</sup> The equation indicates that as the numerator approaches 0 (the samples are not similar), the HQI approaches  $\sqrt{2}$ .

$$HQI = \sqrt{2} \times \sqrt{1 - \frac{K \cdot Q}{\sqrt{K \cdot K} \sqrt{Q \cdot Q}}} \quad (2)$$

K is the known spectrum while Q is the questioned spectrum.

## Principal Components Analysis

Principal components analysis (PCA) is “a variable reduction procedure... [that] reduce[s] the observed variables into a smaller number of principal components that account for most of the observed variance in the variables.”<sup>57</sup> According to O’Rourke, “a principal component can be defined as a linear combination of optimally weighted observed variables.” The principal components are obtained through a singular value decomposition of either a covariance or correlation matrix. The decomposition yields eigenvectors and the associated eigenvalues which are used to calculate the principal components. The first principal component contains the most variance, and each subsequent principal component accounts for less variance and is orthogonal and

uncorrelated to the previous principal component. The number of possible principal components is equal to the number of samples being analyzed. The component loading is the correlation between the component and the variables. Its use does not differentiate between samples per se, only decreases the number of variables which then could be used to conduct further analysis such as a cluster analysis.

It is important in this analysis to identify how many principal components are necessary for subsequent analyses. There are many ways to accomplish this. One is to construct a plot of the eigenvalues associated with each component called a Scree plot and retain all components before there is a break. Secondly, retaining all principal components with eigenvalues greater than one is also another method.<sup>57</sup> The number of principal components that are retained may also be chosen based on the proportion of variance that they account for. However the necessary principal components are determined, they must be valuable to the subsequent analysis and reconstruct the original spectra.

After the number of necessary principal components is determined, the scores associated with each sample can be used to conduct a cluster analysis. The cluster analysis calculates the Euclidian distance between each sample and groups them based on their relative distances. Clusters are formed by joining the two “closest” values together which is then continued in a stepwise fashion until all samples are combined into one single cluster.<sup>58</sup> Such analysis can provide categories based on determined distances but again does not necessarily discriminate between each sample individually. However, there is no guarantee that the main principal components are valuable for discrimination or groupings using further analysis.

## Correlation/Pearson

Similar to the HQI, the Pearson product-moment correlation coefficient value ( $r$ ) is calculated using the following equation,

$$r = \frac{\sum (a_i - \bar{a})(b_i - \bar{b})}{\sqrt{\sum (a_i - \bar{a})^2 \sum (b_i - \bar{b})^2}} \quad (3)$$

In the equation,  $a_i$  is the  $i$ th value in spectrum A and  $b_i$  is the  $i$ th value in spectrum B while  $\bar{a}$  and  $\bar{b}$  are the average values of the spectrum. As the  $r$  value approaches 1, the spectra are considered to be more similar. Normalization of data in this calculation does not affect the outcome as it would in the HQI calculation since the equation involves mean centering the data. However, it is assumed that the variables are measured on an interval- or ratio-level of measurement and that the variables can assume a large number of values.

## Sin<sup>2</sup> $\theta$

Similar to Euclidean distance, the  $\sin^2\theta$  value is calculated using the following equation. This analysis treats each spectrum as a vector and calculates the angle between the vectors.

$$\sin^2\theta = 1 - \frac{(\sum a_i b_i)^2}{(\sum a_i^2 * \sum b_i^2)} \quad (4)$$

## Evaluation: Two-tailed t-test

While calculating values based on comparisons and differences convey how similar or dissimilar samples are, it does not create a way to statistically discriminate between similar comparisons. One way to achieve discrimination between samples is by

using a two-tailed t-test. The t-test is a statistical method used to compare two averages based on their standard deviations. The null hypothesis in this case is that the averages are the same ( $H_0: \bar{x}_1 = \bar{x}_2$ ) while the alternative hypothesis is that they are different ( $H_A: \bar{x}_1 \neq \bar{x}_2$ ). If their distributions overlap significantly (more than the alpha ( $\alpha$ ) value), they are thought to be the same ( $H_0$ ). If they do not overlap significantly, then they are thought to be different ( $H_A$ ).

The averages used during this research were based on same sample comparisons ( $D_{SS}$ ) and different sample comparisons ( $D_{DS}$ ).<sup>59</sup> For example, each sample is analyzed repetitively giving the resultant spectra. The spectra are compared within each sample and averaged over both same sample comparisons ( $D_{SS}$ ) for an individual t-test. Then the spectra are compared between samples and averaged ( $D_{DS}$ ).

Numerically the t-test requires calculating the t value (equation below),

$$t = \frac{|D_{DS} - D_{SS}|}{\sqrt{\frac{S_{DS}^2}{n_{DS}} + \frac{S_{SS}^2}{n_{SS}}}} \quad (5)$$

where  $D_{DS}$  and  $D_{SS}$  are the averages that are defined above and  $S_{DS}$  and  $S_{SS}$  are their standard deviations and  $n_{DS}$  and  $n_{SS}$  are the number of comparisons that were used to calculate the averages, respectively. This calculated t value ( $t_{calc}$ ) is then compared to a t value ( $t_{table}$ ) found in a table which is based on the alpha value and the calculated pooled degrees of freedom (DF).

$$DF_{pooled} = \frac{\left( \frac{S_{DS}^2}{n_{DS}} + \frac{S_{SS}^2}{n_{SS}} \right)^2}{\frac{\left( \frac{S_{DS}^2}{n_{DS}} \right)^2}{n_{DS}-1} + \frac{\left( \frac{S_{SS}^2}{n_{SS}} \right)^2}{n_{SS}-1}} \quad (6)$$

If  $t_{calc}$  is greater than  $t_{table}$ , the samples are statistically different.

### Peak Analysis

Although the entire spectrum is available for comparison, there are some instances when samples only vary by certain elements so that use of the entire spectrum prevents samples from being discriminated from one another due to their overall similarity. Using the peaks from baseline corrected spectra, different spectra from different samples can be compared. Although the resolution of the spectrometers is not accurate enough to assign elements to peaks definitively, numerical data analysis can be employed to gain some discrimination. These methods include the calculation of the Sorenson Index and multivariate analysis of variance (MANOVA) and its subsequent tests (analysis of variance (ANOVA) and Tukey Honestly Significant Difference (HSD) Post-hoc test).

### Sorenson Index

The Sorenson index calculates the similarity between the spectra based on whether they share the same number of peaks.<sup>60</sup> The basic formula can be seen below.

$$S = \frac{2(P_1 \cup P_2)}{P_1 + P_2} \quad (7)$$



where  $P_1$  is the number of peaks in spectrum 1,  $P_2$  is the number of peaks in spectrum 2 and  $P_1 \cup P_2$  represents the number of peaks that the two spectra have in common. As the Sorenson index approaches 1, it is presumed that the spectra are more similar.

### Multivariate Analysis of Variance (MANOVA)

Multivariate analysis of variance is an analysis method in which a multiple criterion variables are evaluated as to their efficacy in differentiating between samples. MANOVA determines “whether there is a significant difference between samples when compared simultaneously on all variables.”<sup>57</sup> In this case, the variables that were evaluated were wavelengths based on the intensity of a peak. Discrimination using MANOVA can be a three part process. The first involves the MANOVA calculations.

The null hypothesis for MANOVA states that all groups have the same mean (M).

$$\begin{pmatrix} M_{11} \\ M_{21} \\ M_{31} \end{pmatrix} = \begin{pmatrix} M_{12} \\ M_{22} \\ M_{32} \end{pmatrix} = \begin{pmatrix} M_{13} \\ M_{23} \\ M_{33} \end{pmatrix} \quad (8)$$

$M_{21}$  indicates the sample mean for the second variable for the first experimental group. A Wilks’ lambda value is calculated based on the matrix of the means to measure the level of association between the variables. An F statistic is calculated to evaluate the significance of the Wilks’ lambda. The formula for the F statistic can be written as

$$F = \frac{MS_{\text{between groups}}}{MS_{\text{within groups}}} \quad (9)$$

MS is the mean square which is a measure of variability.  $MS_{\text{between groups}}$  accounts for variability in error as well as variability due to differences in the means while  $MS_{\text{within groups}}$  accounts for only variability in error.

In the software used during this research, a p value is also calculated that indicates the probability of obtaining an F value greater than or equal to the calculated F value if the null were true. In order to reject the null hypothesis, the p value must be lower than the established significance ( $\alpha$ ) value.

If the MANOVA result is significant (i.e. the groups of means are different), further analysis involving analysis of variance (ANOVA) is performed for each wavelength. ANOVA also calculates a similar F statistic and similarly a p value based upon it which can reject or accept the null hypothesis ( $H_0 : M_1 = M_2 = M_3$ ). ANOVA is comparable to a t-test but it is able to compare more than two samples at a time. It, unlike the MANOVA, can indicate which wavelengths can be used to discriminate between samples.

Finally, if the ANOVA results are significant, the Tukey's Honestly Significant Difference (HSD) test can be employed. The previous two tests only indicate as to whether there were any differences between sample means. This test indicates which samples are statistically different from the others based on their means and can also group them accordingly. However, rejecting the null hypotheses of the previous two tests is necessary in order to perform the Tukey's HSD test.

### Receiver Operating Characteristics Curve

Evaluating a data analysis method can prove to be difficult; however, the use of receiver operator characteristic (ROC) curves has proven successful to evaluate DNA databases. ROC curves originated in clinical medicine trials to provide an objective measure of effectiveness.<sup>61</sup> The analysis evaluates the sensitivity (how close the

differences are) and specificity (whether they can be differentiated) of a data analysis based on comparison values such as HQI values.

The data is ordered into same sample comparisons and different sample comparisons. This analysis assumes that for good sensitivity and specificity each group of values will be different. For instance, in calculating the HQI values for a number of samples analyzed using LIBS, the values for the same sample comparisons should be lower than most of the values for the different sample comparisons. If this were absolute then the area under the curve would be 1.00 and the data analysis would be ideal, i.e. all different sample comparisons would be discriminated from one another. There would be a very low probability that a value from the same sample comparisons would not have a lower score than that from the different sample comparisons. The resultant histogram would have the same sample comparisons grouped near the abscissa, while the different sample comparisons would occupy space above the same sample comparisons. A far from ideal situation would be an area of 0.50. In that case, there would be a 50% probability that the same sample comparison would not have a lower score than that from the different sample comparisons.

### Distribution issues

Many of the data analysis methods that were mentioned previously share a requirement: the data must be normally distributed. A normal distribution is symmetric and has an inherent appeal for those who use it.<sup>62</sup> The appeal encompasses several factors. An addition-based analysis is easier to calculate and understand than a multiplication-based one and results can be stated in a concise manner; the method has been established for more than 100 years; and the distribution retains the title “normal.”

The caveat if the data is not normally distributed is that the results can be misleading and ultimately inaccurate.

It has been suggested and documented that most scientific data is not normally distributed<sup>62</sup> but that the underlying distribution is log normal. This implies that the mean is skewed to the left and values making up the distribution can only be positive. This is the multiplicative (as opposed to the additive: normal) version of the central limit theorem. By taking the log of the values, the distribution can become normal. However, the statistical calculations of the mean, standard deviation, etc. are somewhat different from the normal distribution implied by the multiplicative term.

Another group<sup>63</sup> found that linear correlations between LIBS spectra were gamma distributed. They resolved this issue by averaging sufficient correlation values until the distribution became Gaussian. This phenomenon is further explained and supported in a paper by Gornushkin, et al.<sup>39</sup> Gornushkin also displayed the robustness of linear correlation in regard to peak fluctuations.

Michel and Chave state that LIBS data in particular is not normally distributed.<sup>64</sup> While they cite other researchers in their efforts at obtaining normally distributed spectra, the authors contend that all spectra are representative and should be used. By doing this they conclude that the data does not follow the central limit theorem but rather that LIBS data might follow an extreme value distribution. The authors caution other LIBS users and admonish them to check their data as to normality.

Regardless of the distribution, there are a few different methods to address this problem. One is to convert the data using the Fisher's z transformation and has been used in this research to provide statistically accurate results.

## Fisher's Transformation

Fisher's transformation was developed in 1915 by Fisher for a bivariate distribution. The process converts a non-normal distribution to a normal distribution so that tests that require a normal distribution, such as a t-test, may be performed. The equation can be seen below.<sup>65</sup>

$$Z = \frac{1}{2} \ln \left( \frac{1-r}{1+r} \right) \quad (10)$$

$r$  is the value that is transformed (Pearson coefficient) and  $\ln$  is the natural log. This transformation has classically been used with the Pearson coefficient which often gives a classic bivariate distribution.

## CHAPTER 2: EXPERIMENTAL

### Samples

One hundred ten automotive paint samples were collected from South Carolina Law Enforcement (SLED) and a junkyard in Bithlo, FL (Appendix) over the course of a year. Characteristics of the samples were catalogued and can be seen in the Appendix. Samples ranged a number of production years (1985-2006), makes, manufacturers, and colors. Also noted in the table are the presence/absence of visible effect pigments, type of substrate (if known) and number of discernible layers as seen through a stereomicroscope (34X).

### Instruments

The instrumental parameters for the LIBS instrument for each type of analysis will be detailed in their sections. However, the laser power was maintained at 22 mJ/pulse except during the cross section reproducibility experiments when it was at 31 mJ/pulse. The Q-switch delay was optimized for each experimental day and varied between -2.5 and -5.0  $\mu\text{s}$ . The atmosphere was air at ambient pressure and temperature.

The second instrument used during this research, the ATI Mattson Infinity Series FTIR with a SpectraTech IR Plan Advantage IR Microscope using an ATR objective, was used to obtain FTIR spectra of the samples. Spectra were processed and analyzed using the OMNIC software.

Finally the LEO 1450VP Scanning Electron Microscope equipped with an Oxford Energy Dispersive Spectrometer was used to obtain X-ray spectra of the cross sections of

the samples. The INCAEnergy Microanalysis System software was used to analyze the spectra from each sample.

### Analysis

Table 2 details the experiments performed for this research that are further explained below.

Table 2. Summary of details of research experiments

Experiment	Instrument	Cross Section (CS) / Drill Down (DD)	Number of samples	Spectra per sample	Set	Sample preparation	Time after initial experiment
1	LIBS	CS	25	5	1	chip	
2	LIBS	CS	51	5	1	chip	
3	LIBS	CS	10	5	2	chip	0
4	LIBS	CS	10	5	2	chip	2 days
5	LIBS	CS	10	5	2	chip	1 week
6	LIBS	CS	10	15	2	chip	4 weeks
7	LIBS	DD	25	20	1	substrate	
8	LIBS	DD	25	20	2	chip	
9	LIBS	DD	93	20	1	chip	
	FTIR-ATR		51	3	1	substrate	
	SEM/EDS	CS	23	3	1	chip	

### LIBS

The inherent structure of the layers of a paint chip allows for two different methods of approaching its analysis: from the top using a drill down method or from the edge analyzing the cross section (Figure 7).

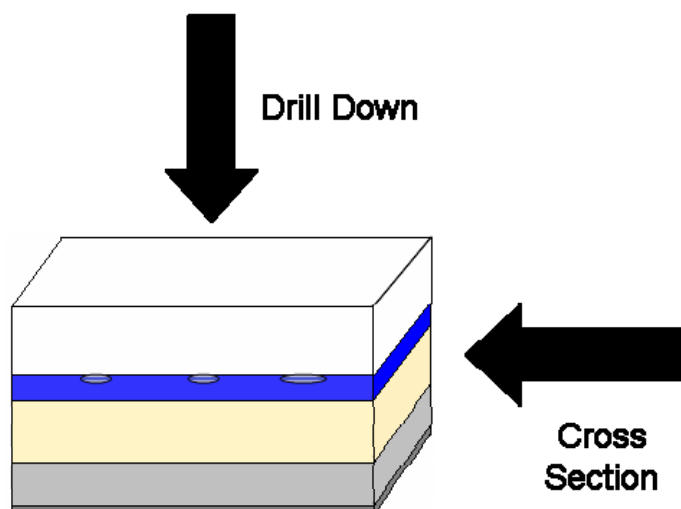


Figure 7. Two analysis methods

### Cross Section

The first method was interrogating the edge or cross section of the paint chip. Figure 8 depicts the sample setup of the cross section analysis. Two microscope slides were employed to keep the paint chip normal to the surface of the stage. Double sided tape was used to keep the microscope slides in place. All layers were simultaneously analyzed in one pulse.

Five spectra per sample were obtained for analysis for both Experiment 1 and 2. For the reproducibility tests (Experiments 3, 4, 5 and 6), a chip from a sample was split in half and five single shot spectra were obtained from the edge of each resulting chip (Experiments 3, 4 and 5). The splitting of the chip created two sets of data: spectra from the first chip (Set 1) and spectra from the second chip (Set 2). The time between analyses 3 and 4 was two days and between 3 and 5 was one week. For analysis 6, a chip from each sample was split in half as with the previous analyses; however, fifteen spectra from



each chip were used for the analysis. The time between experiments 5 and 6 was three weeks.

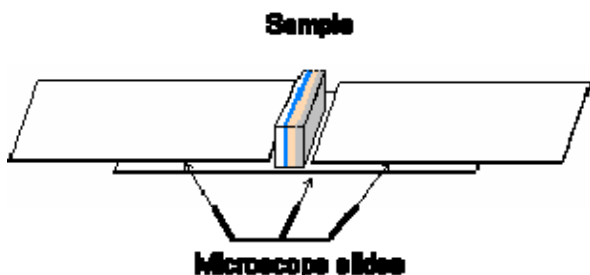


Figure 8: Cross Section Analysis (paint chip not drawn to scale)

### Drill Down

The second method of analysis involved drilling down through the layers starting with the clearcoat. Two different arrangements were designed for this type of analysis. The first was the most straightforward and required analyzing the paint chip on its substrate, if present, and drilling down from the top (clearcoat) down to the substrate (Appendix: LIBS Drilldown, Experiment 7). Twenty single pulse spectra were saved using this setup. Five different locations (spots) on the sample were analyzed per sample. This analysis was only performed on the first 25 samples.

The second arrangement involved only the paint layers which were mounted on polyisobutylene on a microscope slide (Figure 10). The polyisobutylene had been softened at  $\sim 200^{\circ}\text{C}$  and smoothed so that the paint chips would lay flat. At great enough thicknesses, isobutylene does not produce a signal during the LIBS experiment (Figure 9), and it imparts stability to the samples during the analysis.

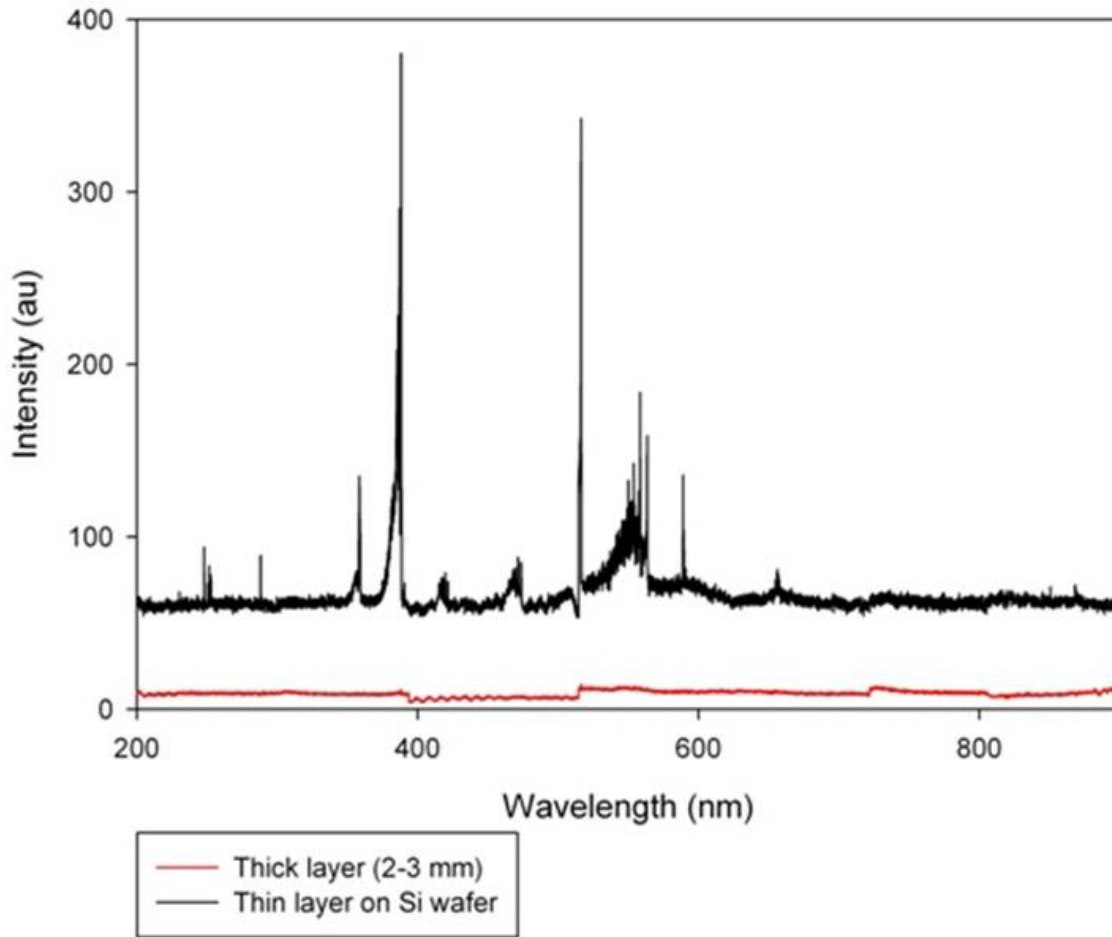


Figure 9. Spectra of polyisobutylene at different thicknesses

If samples were attached to a substrate, a large enough chip was removed for analysis.

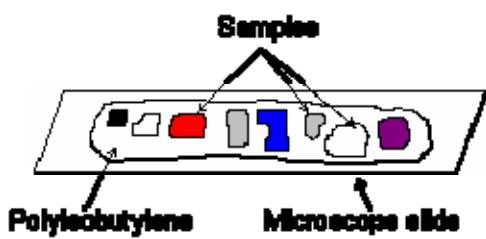


Figure 10. Drill Down Analysis

A preliminary drilldown was performed in order to determine the number of pulses necessary to go through all the layers. The spectra from each subsequent drilldown were averaged by the software and three spectra from each sample were obtained. The number of shots per drill down varied between chips. An initial analysis was performed in which two chips each from 25 samples were analyzed (Appendix: LIBS Drill Down, Experiment 8). Three spectra from each paint chip were acquired. A second analysis involving ninety-three samples was also conducted using this arrangement (LIBS Drill Down, Experiment 9).

#### FTIR-ATR

The clearcoats of fifty-one samples were analyzed using the FTIR-ATR (microscope). The samples were placed on a microscope slide on a pressure sensor plate on the stage of the microscope, and the stage was adjusted so that sufficient pressure was applied between the silicon crystal of the ATR and the sample. Three spectra of 32 scans each were obtained from different locations on the surface of the sample. The absorbance spectra were taken from  $4000 - 650 \text{ cm}^{-1}$ .

#### SEM/EDS

The spectra from the cross sections of 26 samples (SEM/EDS: Appendix 1) were obtained using the SEM/EDS. Thin layers of the cross section from the samples were cut using a scalpel. These were placed on an adhesive carbon tab which was mounted on an aluminum stub (Figure 11). The samples were lightly sputtered with carbon with the Denton Vacuum LLC Desk II Cold Sputter/Etch Unit and Carbon Evaporation Accessory

(Denton Vacuum Inc.) to prevent charging of the sample before placing in the sample chamber of the SEM/EDS.

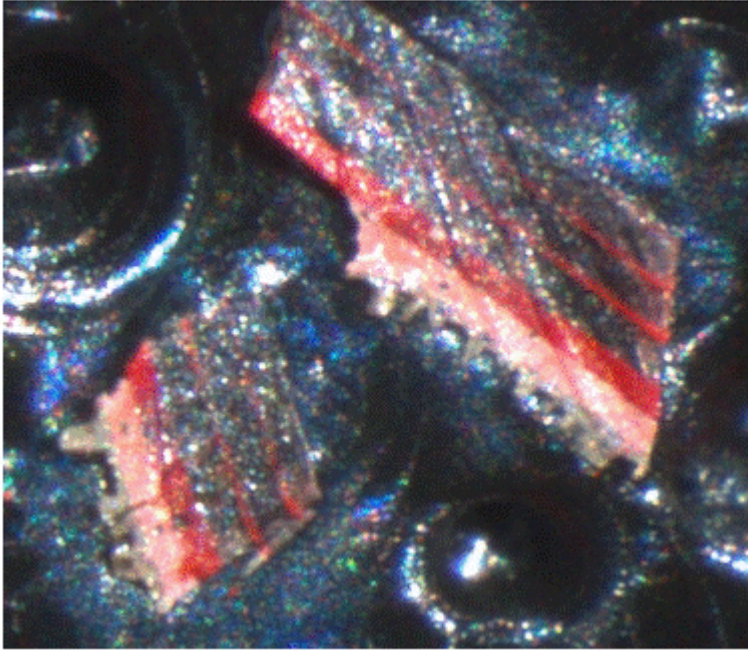


Figure 11. Stereomicrograph (50.4X) of sample preparation for SEM/EDS analysis

The working distance of the SEM was maintained at 15 mm while the accelerating voltage for EDS analysis was 20 keV. The beam current was varied based on the sample in order to maintain an acquisition rate of 2-3 kilocounts per second (kcps). A strip of copper was used as the standard for quantitative optimization.

## CHAPTER 3: LIBS Cross Section

Five spectra each from three samples can be seen in Figure 12. Each spectrum is representative of the different types of spectra obtained from the LIBS cross section analysis. The number of peaks that can be observed in the 03 Saturn Ion spectra (a) is much greater than that in the spectra from the 02 Ford Mustang (c). The 95 Honda Civic (b), on the other hand, appears to have two spectra with many peaks and three spectra with very few peaks. This inconsistency between the spectra from the same sample will become important later during the numerical/statistical analyses.

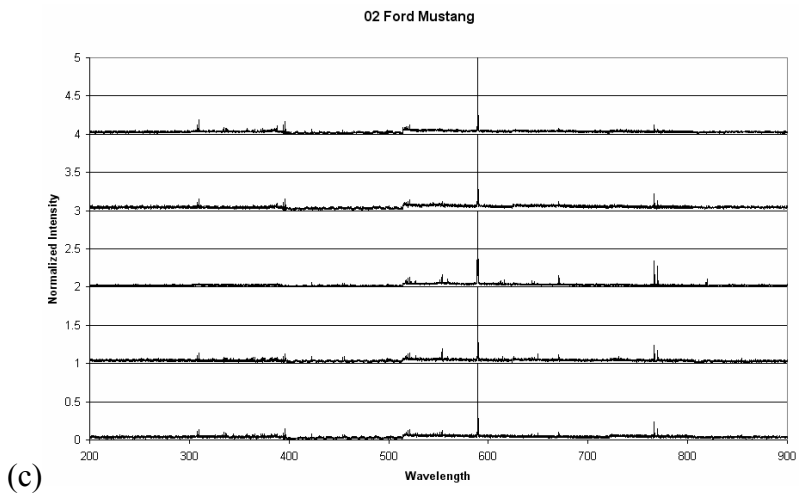
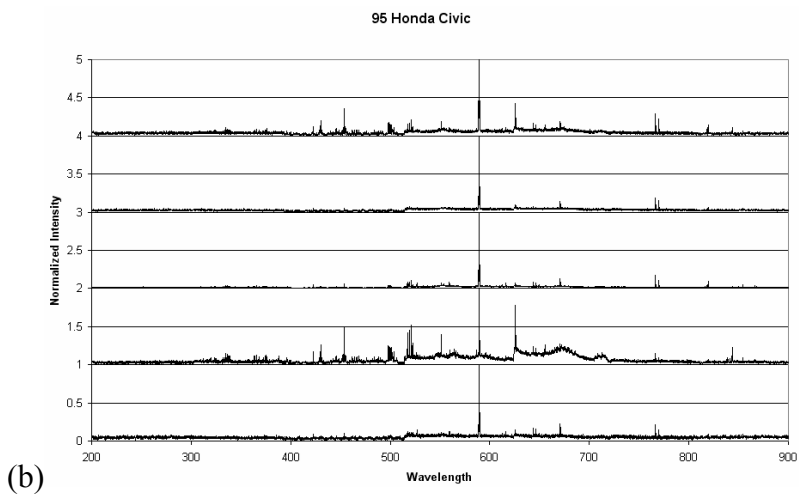
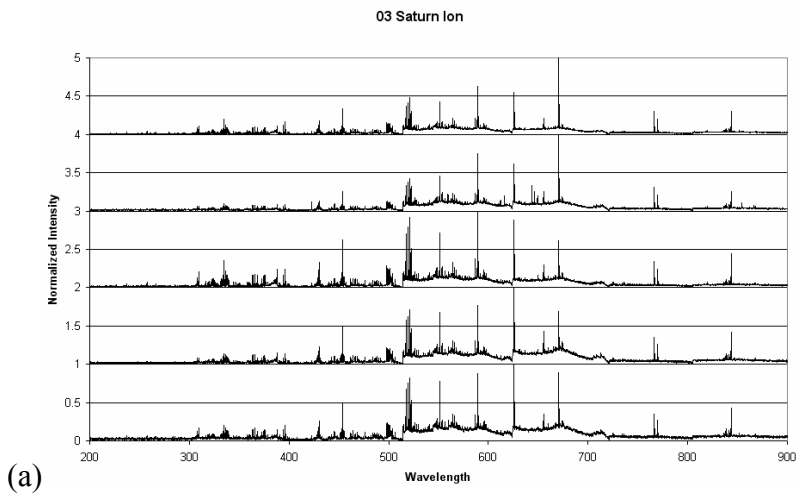


Figure 12. Normalized spectra from three samples from the cross section analysis

## Library

Each of the single shot spectra from Experiment 1 (Appendix: LIBS Cross Section) were compared to each other using the HQI equation (Eqn. 2). The same sample HQI comparison values and the different sample HQI comparison values calculated between the spectra were used to conduct a ROC analysis (SigmaPlot 10.0). The ROC analysis (Figure 13) revealed the usefulness of this type of analysis. The area under the curve was 0.92 which indicated that there was a 0.92 probability that the HQI value between two randomly chosen spectra from the same sample (Correct) would be smaller than the HQI value between two randomly chosen spectra from two different samples (Incorrect). As can be seen, the HQI values for the same sample comparison (Correct) varied widely, reaching values as high as 0.75.

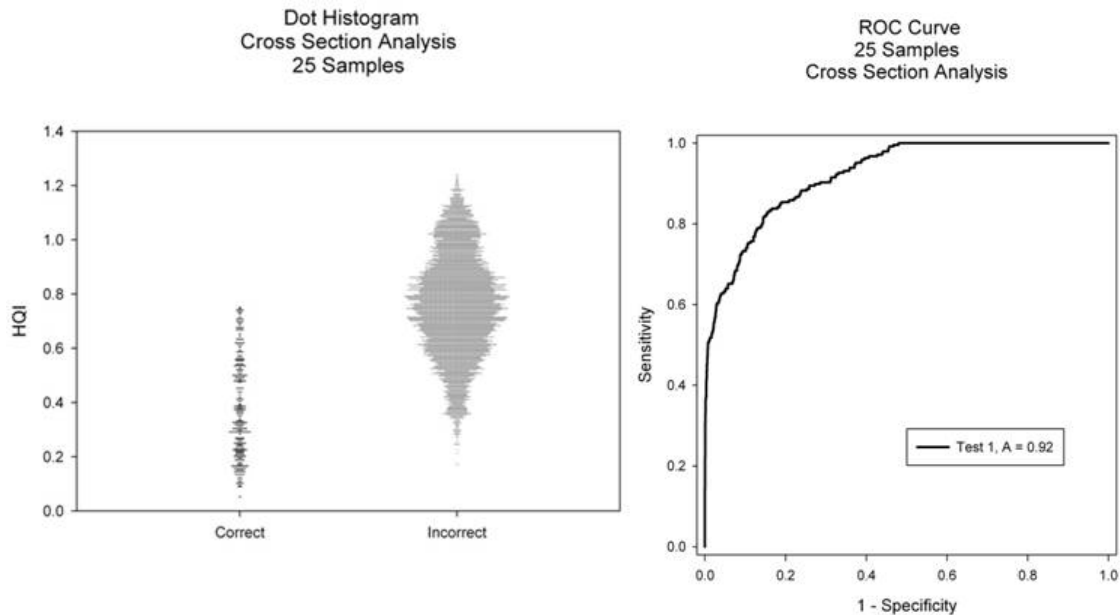


Figure 13. ROC analysis of replicate cross section analyses

## HQI and t-test

The HQI values for comparisons between spectra were calculated for both Experiments 1 and 2 together and separately and compared using a t-test to determine whether the samples could be discriminated from each other. The  $\alpha$  value was held at 0.05 and the results can be seen in Table 3 for each analysis. The sample set 2<sub>25</sub> indicates the twenty-five samples that were analyzed during Experiment 2 that were also analyzed during Experiment 1. Of the 25 samples that were repeatedly analyzed, only 12% (3 of 25) of same sample comparisons were not discriminated from themselves.

Table 3. Results from the HQI/t-test cross section analysis

	Different Sample Discrimination	Same Sample Discrimination
1 v. 2 <sub>25</sub>	95.2%	88.0%
2 v. 2	92.9%	
1 2 v. 1 2	95.4%	88.0%

The high same sample discrimination from the t-test can be illustrated by examining the  $D_{DS}$  and  $D_{SS}$  distributions for the same sample comparison of sample 18 (Figure14). The standard deviations appeared similar but the averages were far enough apart that the two curves did not overlap significantly to be considered statistically similar.



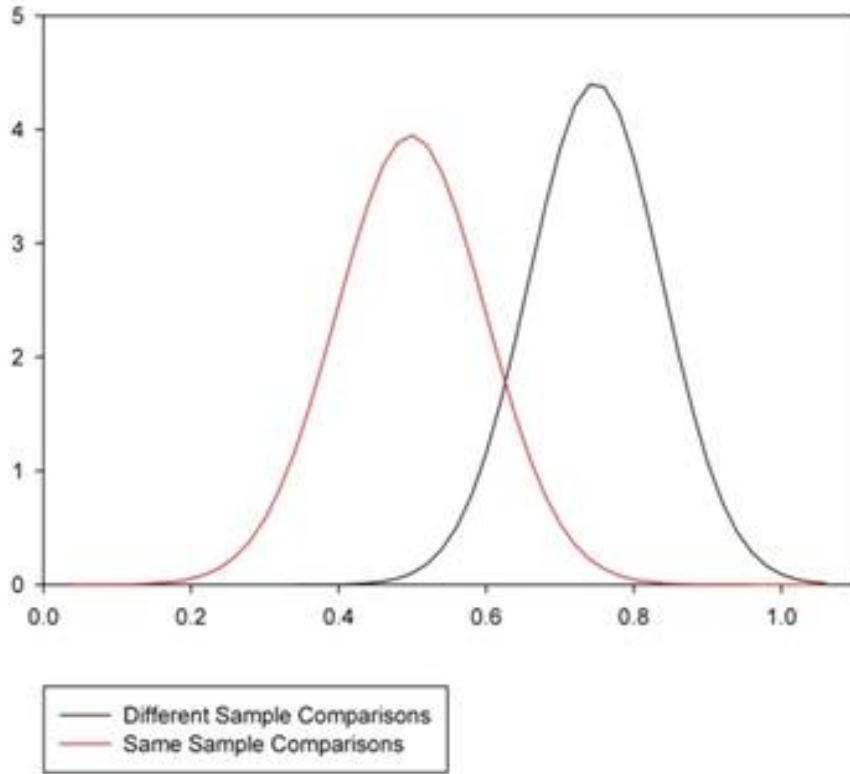


Figure 14. Distribution of same sample comparison and different sample comparison for t-test

Reproducibility tests

In order to explore the large amount of Type I error (discrimination between samples that should not be discriminated) found in the previous analyses, the spectra of ten samples (Appendix: LIBS Cross Section: Experiments 3, 4, 5 and 6) were compared using t-tests based on HQI values. Tables 4 and 5 give the results of these experiments.

Table 4. Different sample discrimination of reproducibility experiments

Different Sample Discrimination	Experiment			
	3	4	5	6
3	98.3			
4	99.4	100		
5	100	99.4	98.9	
6	89.5	90.0	89.5	100

Table 5. Same sample discrimination of reproducibility experiments

Same Sample Discrimination	Experiment			
	3	4	5	6
3	50			
4	72.5	60		
5	62.5	62.5	50	
6	92.5	62.5	62.5	90

From two days to a week after the initial experiment, the discrimination between samples increased slightly from 98.3 to 100%. There was a significant drop of discrimination between different samples between the experiments run within a week (3, 4 and 5) and after four weeks (6). The same sample discrimination, which is initially high as well, also increased after two days or a week with the largest amount of same sample discrimination (92.5%) between Experiment 3 and 6.

When the fifteen spectra from Experiment 6 were averaged ( $15/5 = 3$  spectra), the discrimination between different samples decreased to 85.8% while the same sample discrimination also decreased to 80%.

## Discussion

The results from the Library data analysis showed a 0.92 area under the curve for the ROC analysis and indicated that this type of data analysis might be suitable for LIBS cross section paint data. Although the area was relatively high, the dot histogram also revealed that the same sample HQI values reached as high as 0.75 and did not group well near the abscissa. This might be an indication of poor reproducibility of the cross section spectra.

HQI/t-test showed mixed results. While the discrimination for comparisons between different samples using the HQI/t-test is rather high, the same sample discrimination was also high which is unacceptable in this case. Even when the number of spectra per sample was increased, the same sample discrimination also increased leading to 90% of the samples being discriminated from themselves. This high self discrimination calls into doubt the discrimination between the samples since it greatly exceeds the alpha value.

This irreproducibility could be due to a variety of different factors originating from both instrumental and sample issues. These issues could include laser variability, layer thickness, orientation of the sample and heterogeneity within the sample. Although the laser power level was set on the power supply of the laser, there are slight fluctuations of the laser pulse power from pulse to pulse.

Optical considerations could also contribute to poor reproducibility. They proved to be important for cross section analysis since the area of sampling was small. If the laser was not directly focused on the same point in the cross section each time it was pulsed, the spectra could be different as the LIB event consumed different amounts of

each layer. If the surface of the cross section was not at the same angle to the laser beam, the spectra could also be different due to problems with focusing the camera used to image the sample area that was ablated. These were issues that could possibly have influenced the reproducibility when sampling from the cross section of the paint sample. Without pinpointing the cause, the sample-to-sample irreproducibility of the data makes the cross section sampling method unusable.

## CHAPTER 4: LIBS DRILL DOWN

An image of the laser profile on burn paper was obtained and can be seen in Figure 15. The ablation from the energy level used during the drill down experiments is situated second from the right. The ablation was not circular and “tailed” in one direction. As the power was increased, the ablation became more circular (leftmost ablation).

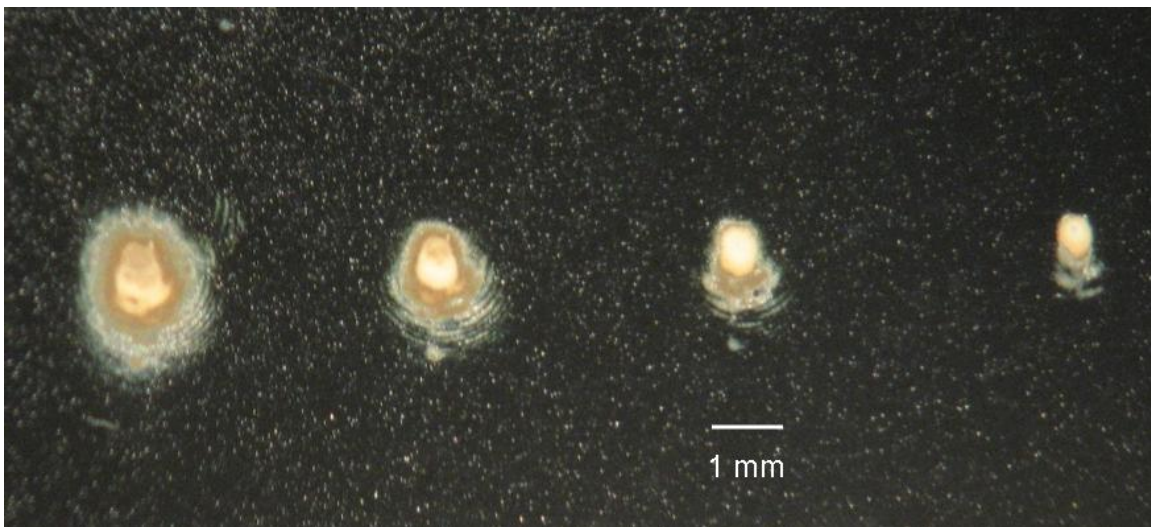


Figure 15. Micrograph of laser ablation of burn paper at decreasing laser energy levels

With the same energy (22 mJ/pulse), an automotive paint sample was ablated with one laser pulse (Figure 16). The pulse ablated both the clear coat and basecoat (large circle in red) down to the surfacer layer (smaller red circle). Again the ablation was not circular.

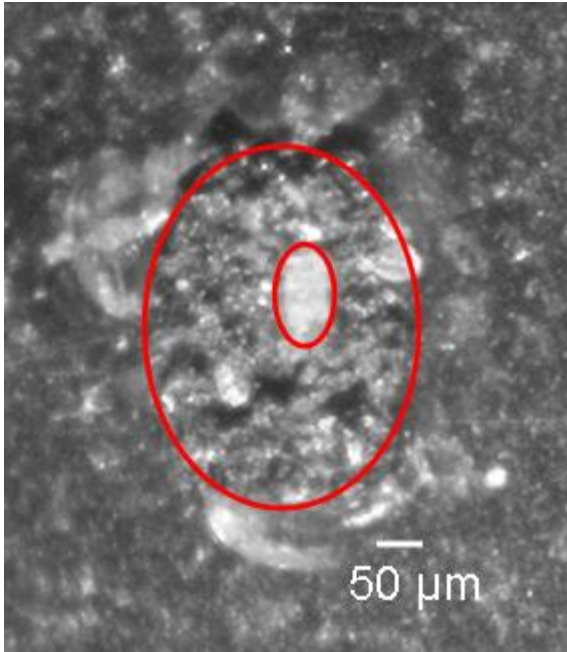


Figure 16. Micrograph of the crater formed from a single laser pulse on a paint sample

Other observations of the ablation of the paint sample (Figure 16) include the distribution of the effect pigments within the basecoat. In the micrograph, the distribution does not appear homogeneous while different types of effect pigments appear to be present (blue and white colors not seen in image). The diameter of the laser is obviously larger than the pigments themselves.

A raw drill down spectrum from samples 90 and 33 can be seen in Figure 17. Although the samples share certain attributes (color and presence of effect pigments), their spectra are visually different.

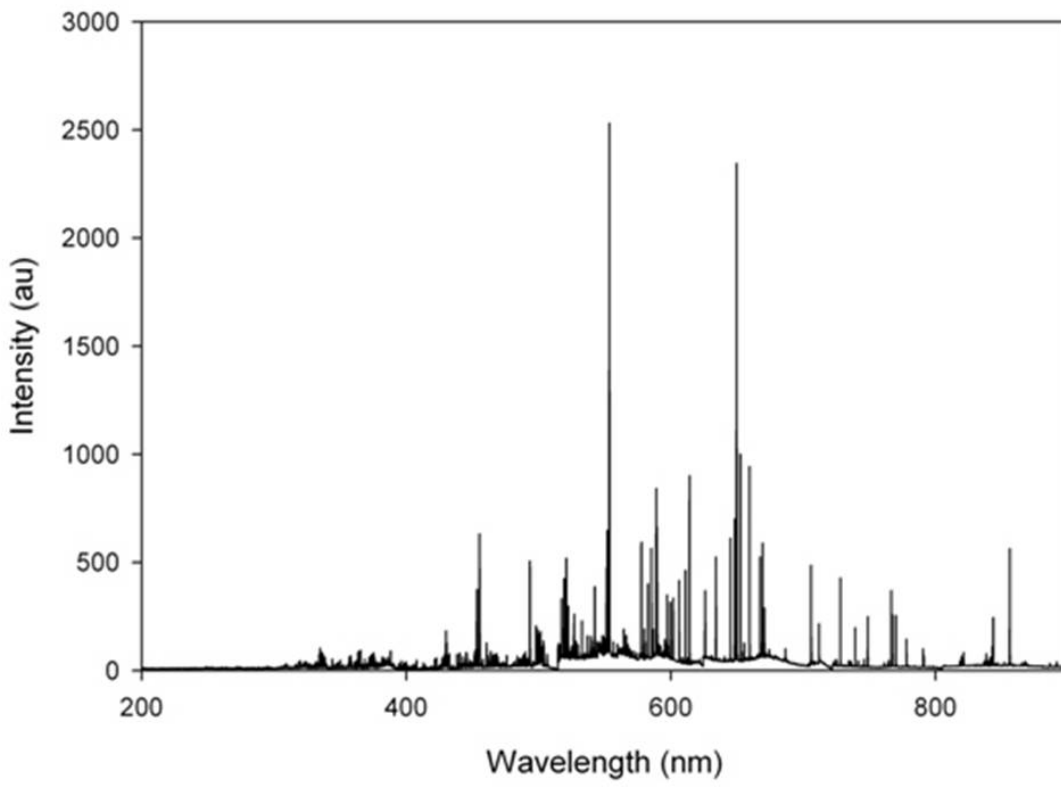
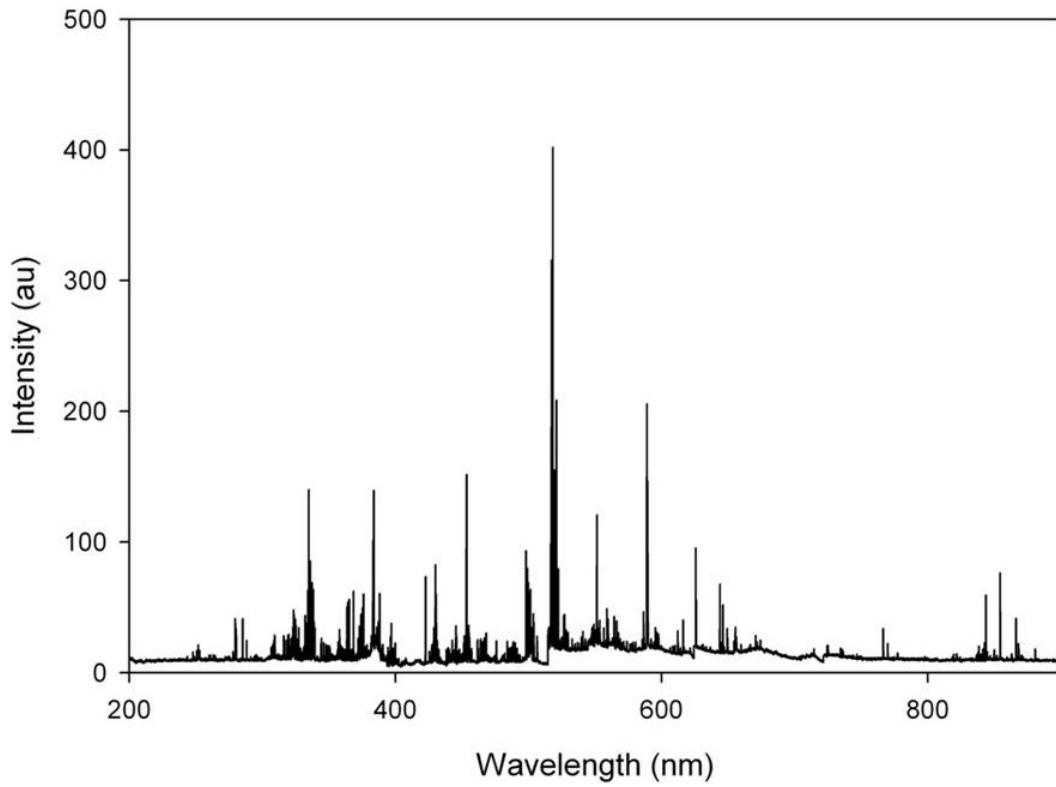


Figure 17. Averaged drill down spectra of 1987 Dodge Ram (a) and 2005 Mazda Tribute (b)

The drill down analyses will be divided into two different categories based on how the samples were prepared. The first set of samples that will be discussed was analyzed on their substrate (if present) and the second set was analyzed on polyisobutylene.

### Substrate

The samples included for this data analysis are only from the LIBS Drill Down, Experiment 7 group (Appendix).

### Layer Identification

Pearson correlation values were calculated between spectra from the same location on the same sample. A matrix of the Pearson correlation values between the spectra within a single drill down was constructed for each location on each sample. Contour surface plots were constructed based on the matrix of these Pearson correlation values for each location of analysis. By comparing each spectrum within the same drill down, distinctions between each individual layer may be found. In Figure 18, the plot on the right is an example of a sample that was “well behaved,” meaning that there appears to be distinctions between the spectra. There are spectra that correlate more highly with each other than the other spectra designating them as coming from the same layer. The plot on the left is not a “well behaved” sample; there is high correlation between all the spectra for the sample and there does not appear to be any discernible layers.



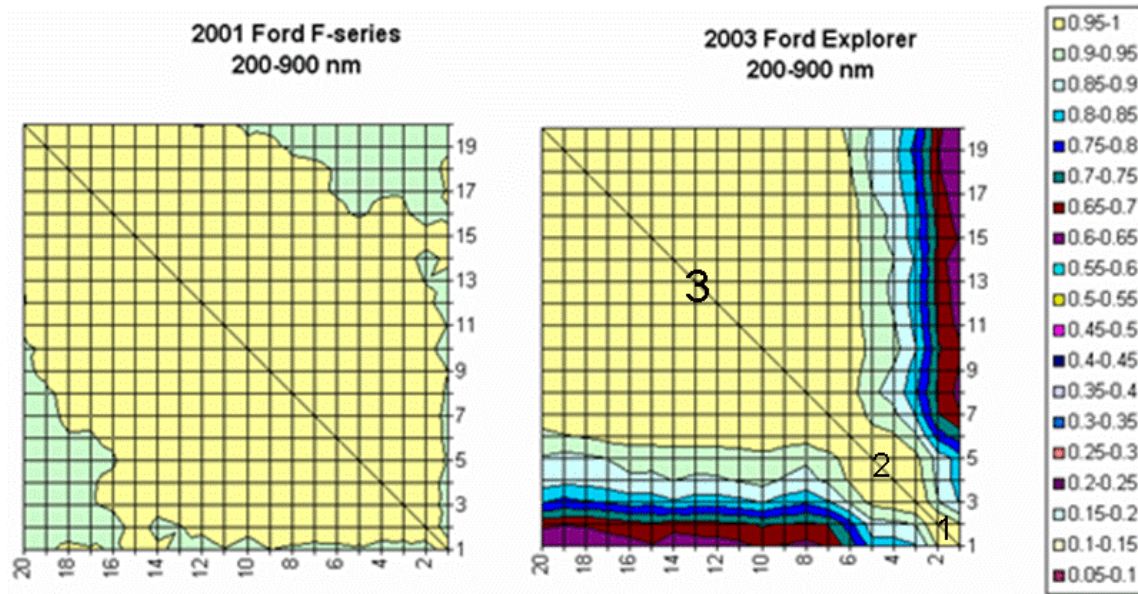


Figure 18. Contour surface plots based on Pearson correlation values comparing spectra within the same drill down.

### Library

Based on the results from the previous data analysis, the first five spectra from each location on each sample were averaged giving five averaged spectra per sample. The resultant averaged spectra were compared to each other using the HQI equation (2). The same sample comparison values were separated from the different sample comparison values and a ROC curve analysis was performed. The ROC curve and histogram for the results of this analysis (Figure 19) showed the relatively good sensitivity and specificity of this method of analysis. The area under the curve was 0.98 and there was relatively little overlap between the Correct and Incorrect values based on the dot histogram.

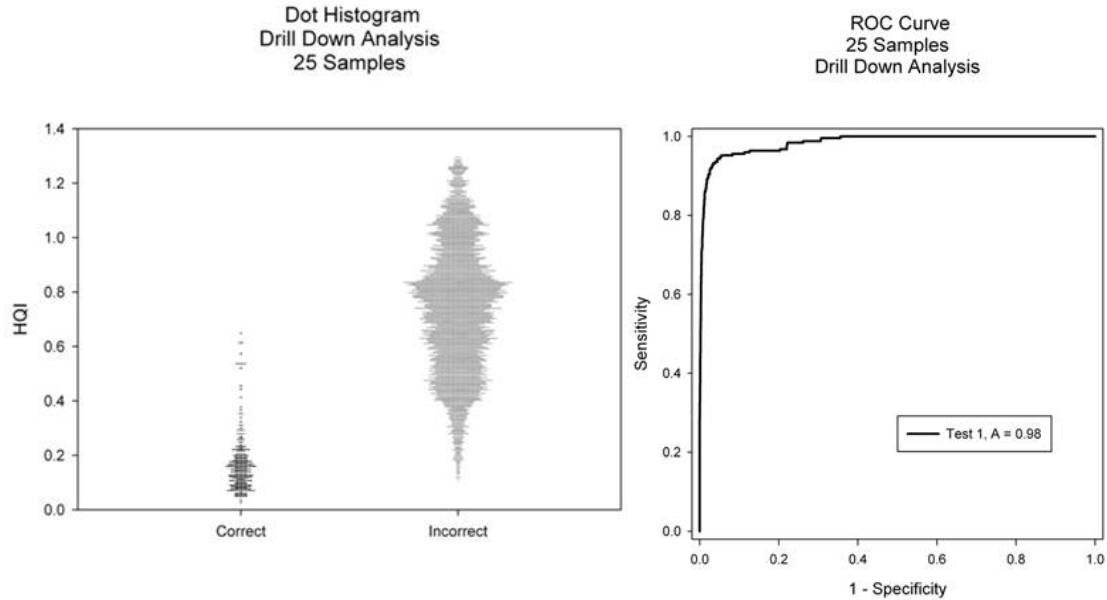


Figure 19. ROC analysis of Library analysis of drill down spectra

### Polyisobutylene Mounted Analyses

The spectra from Experiments 8 and 9 were the basis for the following data analyses. Spectra from both experiments were used to conduct full spectrum analyses while the spectra from Experiment 8 were also used for peak analysis.

#### Full Spectrum

While a full spectrum obtained using LIBS encompassed the range of 198 to 965 nm, only the data from 200 to 900 nm were used for data/statistical analysis.

#### t-test

The spectra from both Experiments 8 and 9 were the basis for this analysis. Two different values based on the full spectrum were calculated for subsequent t-tests: HQI and the Fisher transform of the Pearson correlation coefficient ( $Z(r)$ ). Both calculated

types of values entailed using the full spectrum however the spectra were normalized prior to calculation of the HQI. Using the HQI equation, values were calculated for comparisons between the spectra. Two-tailed t-tests were performed based on the HQI values calculated between and within samples.

Table 6. T-test results based on HQI values from drill down spectra

Experiment	No. of samples	No. of spectra per file	No. of shots per spectrum	Different Sample Discrimination (%)	Same Sample Discrimination (%)
8	25	3	variable	95.0	16.0
8 (BC)	25	3	variable	94.5	12.5
9	93	3	variable	99.4	
9	93	3-5	variable	99.2	
9 (BC)	93	3-5	variable	99.3	

BC: Baseline corrected spectra

In Table 6, “variable” indicates that the number of spectra per averaged spectrum was determined during the initial drill down. Baseline correcting (BC) the spectra did not appear to change the different sample discrimination while the same sample discrimination decreased. Increasing the number of spectra per file decreased different sample discrimination only slightly (99.4 to 99.2).

The other value that was calculated before further t-tests were performed was Pearson’s correlation coefficient. After calculation of the value of r it was converted using Fisher’s transformation ( $Z(r)$ ), and the t-test was performed on the  $Z(r)$  values. Table 7 shows the results of the various data analyses.

Table 7. T-test results based on Z(r) values from drill down spectra

Experiment	No. of samples	No. of spectra per file	No. of shots per spectrum	Different Sample Discrimination (%)	Same Sample Discrimination (%)
8	25	3	variable	95.5	20.0
8 (BC)	25	3	variable	95.3	12.0
9	93	3	variable	94.9	
9	93	3-5	variable	99.6	
9 (BC)	93	3-5	variable	99.7	

BC: Baseline corrected spectra

Similar results were obtained with the Z(r) values as with the HQI values.

Baseline correcting the spectra allowed for less discrimination between same sample comparisons. However, using more spectra per file allowed for better discrimination with t-tests based on the Z(r) values while baseline correcting the spectra had a mixed result between the different sample comparisons between the two different set sizes.

#### PCA/Cluster Analysis

The twenty-five samples utilized for this analysis can be seen in the Appendix (LIBS Drill Down, Experiment 8). Spectra were first normalized and then averaged prior to analysis. Non-baseline corrected spectra were normalized by two separate methods. The first method involved dividing each intensity in a spectrum by the square root of the sum of the squares of the intensity in the spectrum ( $\sqrt{\sum x_i^2}$ ) while in the second method the intensity was divided by the sum of the intensities within the spectrum ( $\sum x_i$ ). Baseline corrected (BC) and non-baseline corrected (NBC) spectra were analyzed separately. Using the Mathematica software, the data matrix (rows x columns = wavelengths x sample) was premultiplied by its transpose and the eigenvalues and eigenvectors were obtained by decomposition of the matrix.

Two different methods for determining the necessary number of principal components were used. A Scree plot and any eigenvalue greater than 1 were evaluated as to their effectiveness. The Scree plot for the first set of non-baseline corrected spectra normalized using the first method (Figure 20) indicated the first three components while the eigenvalue  $>1$  method indicated seven components. The first three components accounted for 99.1% of the variance while seven components accounted for 99.7%.

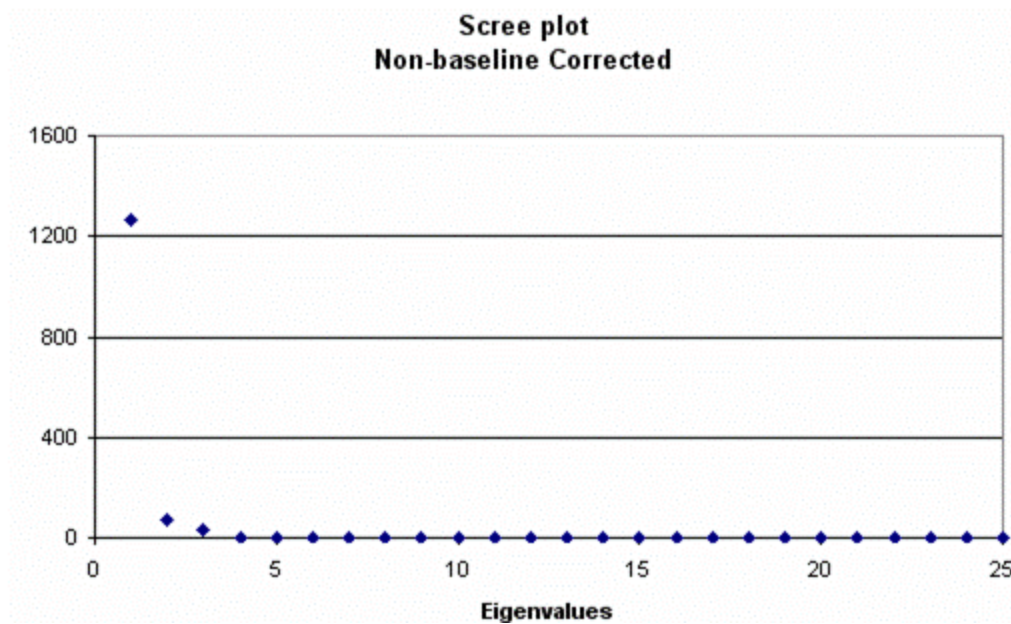


Figure 20. Scree plot of eigenvalues from PCA of non-baseline corrected spectra

For further investigation, the eigenvectors associated with these methods were examined using a cluster analysis. The dendrogram from the cluster analysis based on each set of eigenvectors is displayed in Figure 21. Around a distance of 1.0, there are five different groups based on 3 eigenvectors (top). When 7 eigenvectors (bottom) are used, the distance drops to 0.8. However, the constituents of the different groups did not change from increasing the number of eigenvectors used for the analysis.

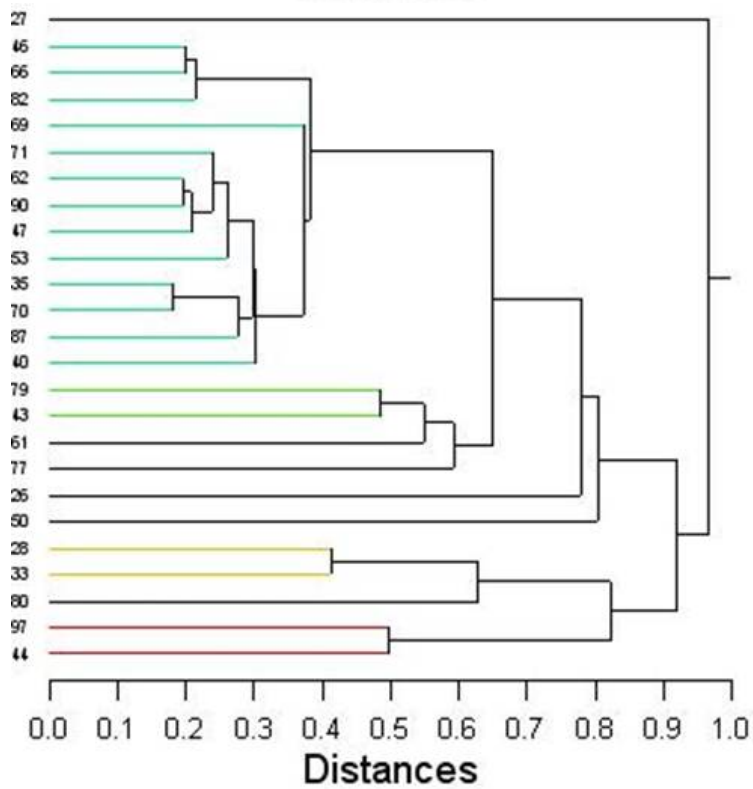
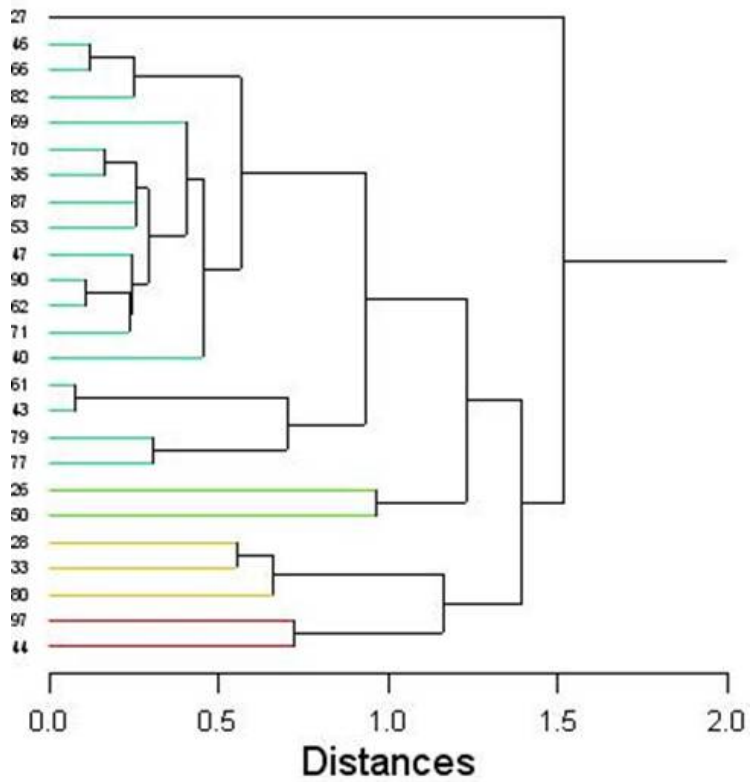


Figure 21. Cluster analysis dendograms based on principal components (3: top; 7: bottom) based on NBC spectra

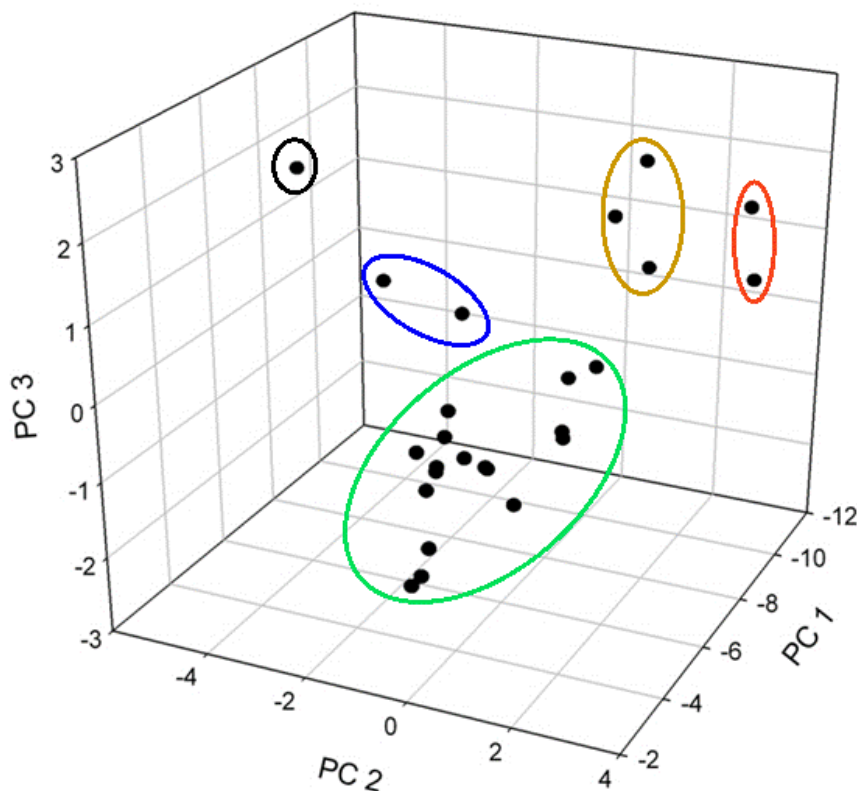


Figure 22. Principal components plot based on PCA of NBC spectra

The plot of the first three principal components (Figure 22) for each sample shows the groupings based on the cluster analysis. Although there did appear to be some smaller groupings within the largest grouping (circled in green), the distances between these small groupings were smaller than the distances between the other groupings (black, blue, gold and red). The circled groupings in Figure 22 were hand drawn and do not indicate 95% confidence ellipses. The samples within each grouping did not correspond to any association based on year, manufacturer, physical characteristics, etc.

When the spectra were normalized by the second method, none of the eigenvalues were greater than one so the necessary eigenvalues were determined through the Scree

plot (Figure 23). The plot indicated that three eigenvalues were valuable for later analysis and that they made up 99.2% of the variance within the spectra.

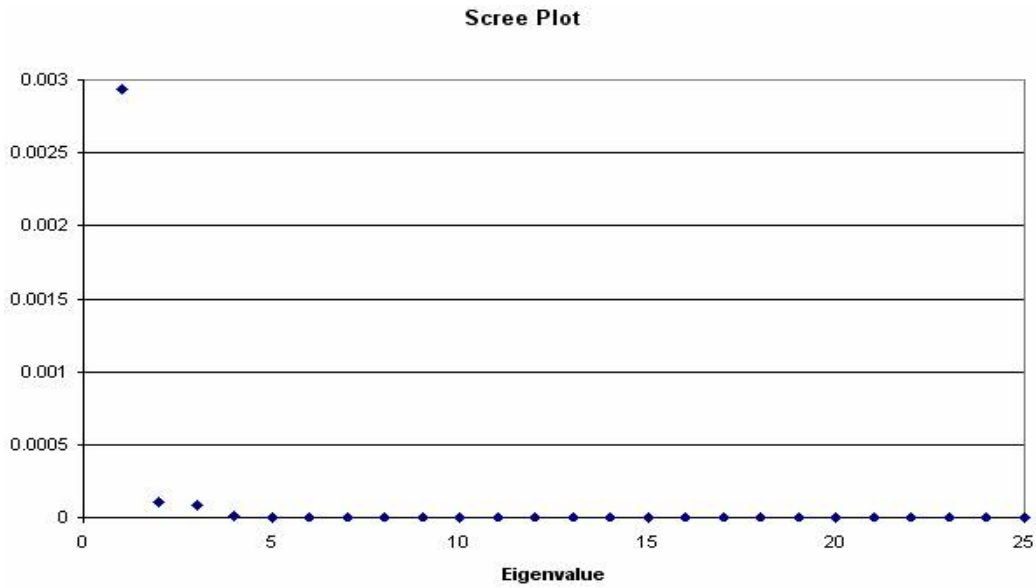


Figure 23. Scree plot of eigenvalues based on PCA of NBC spectra normalized by the 2<sup>nd</sup> method



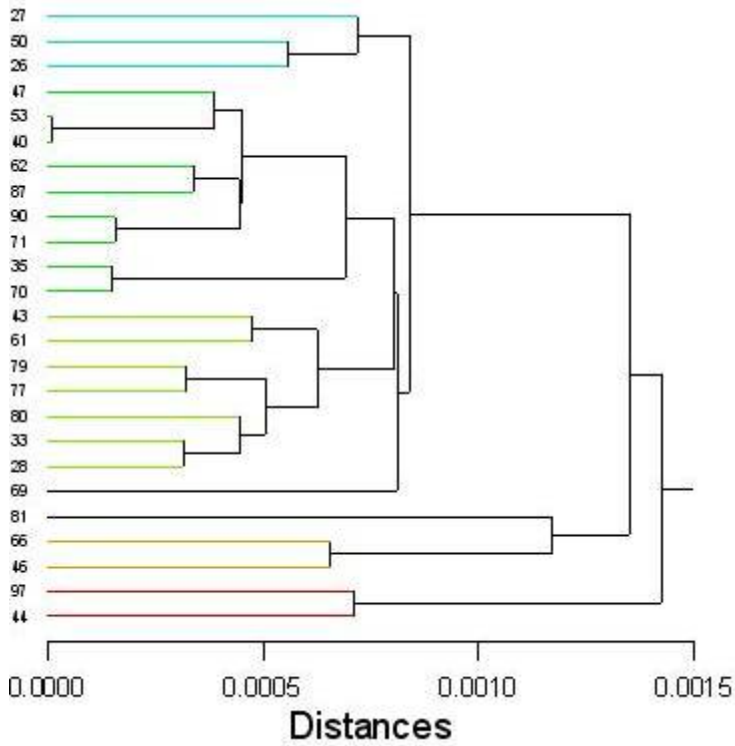


Figure 24. Cluster analysis dendrogram of 3 principal components based on NBC spectra

The cluster analysis revealed four different groups at a distance of 0.0010 (Figure 24). These groups have been identified in the plot of the three principal components (Figure 25). Again, smaller clustering can be seen within the largest group and samples within the groups can not be associated based on their model, physical characteristics, etc.

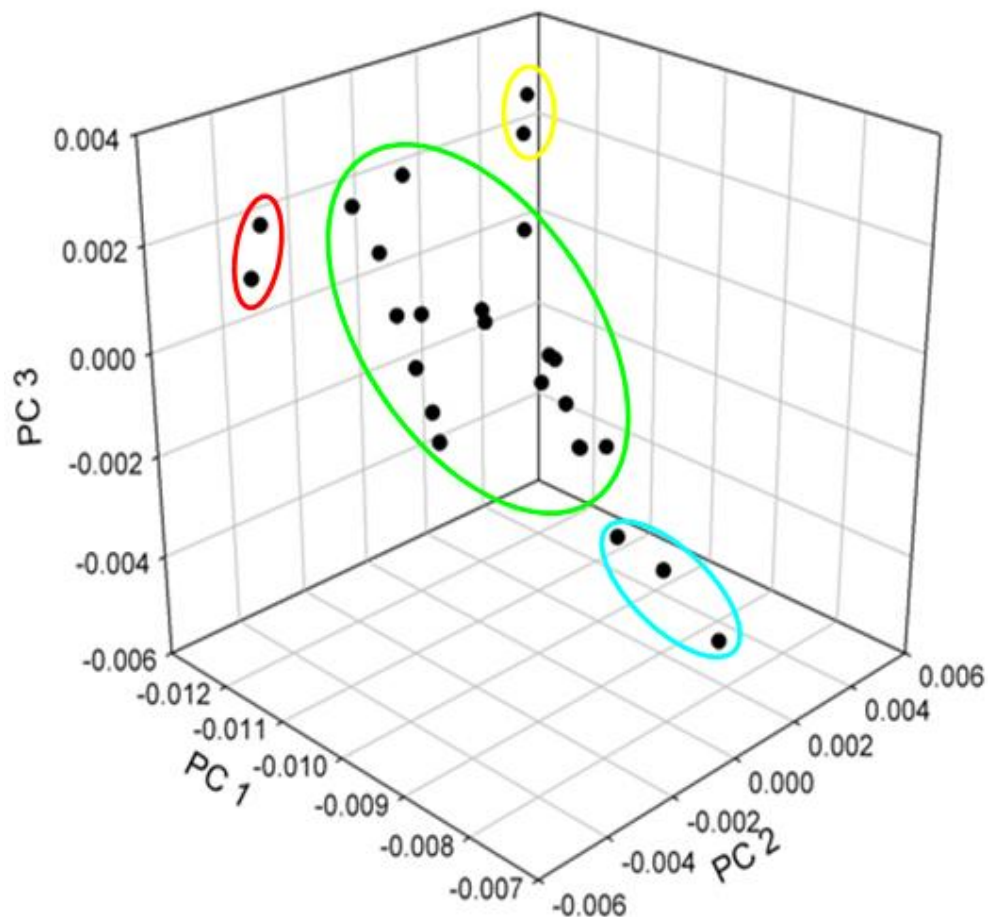


Figure 25. Plot of three principal components obtained from PCA of NBC spectra

Baseline correcting the spectra produced different results. The significant eigenvectors based on the Scree plot was four (97.0 % of the variance) while those based on the >1 method was five (97.8% of the variance). Cluster analysis revealed some similarities with the NBC spectra (Figure 26). For example, samples 28 and 44 are still relatively close to each other and there was a large grouping (green) that was important in the previous cluster analyses.

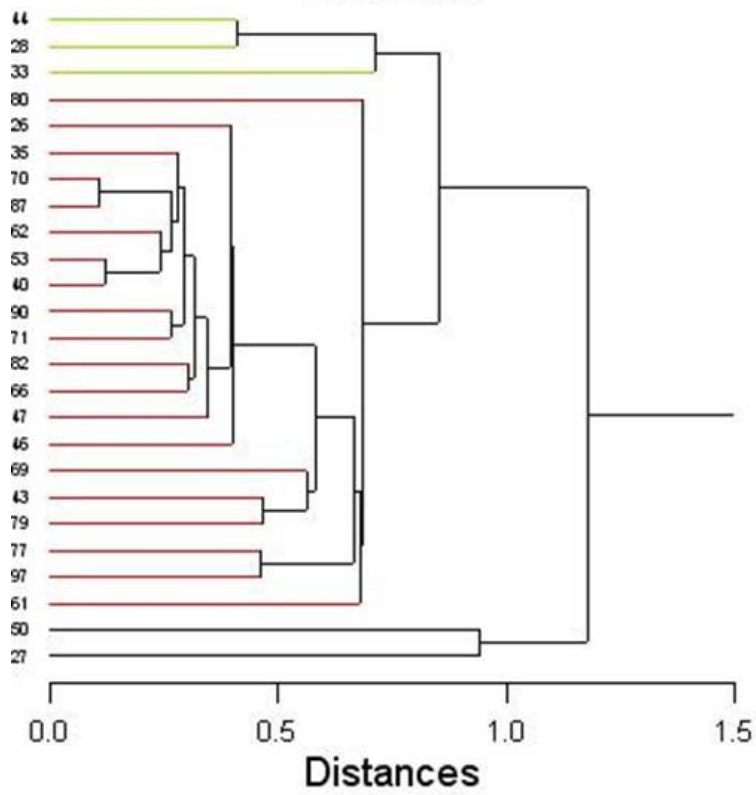
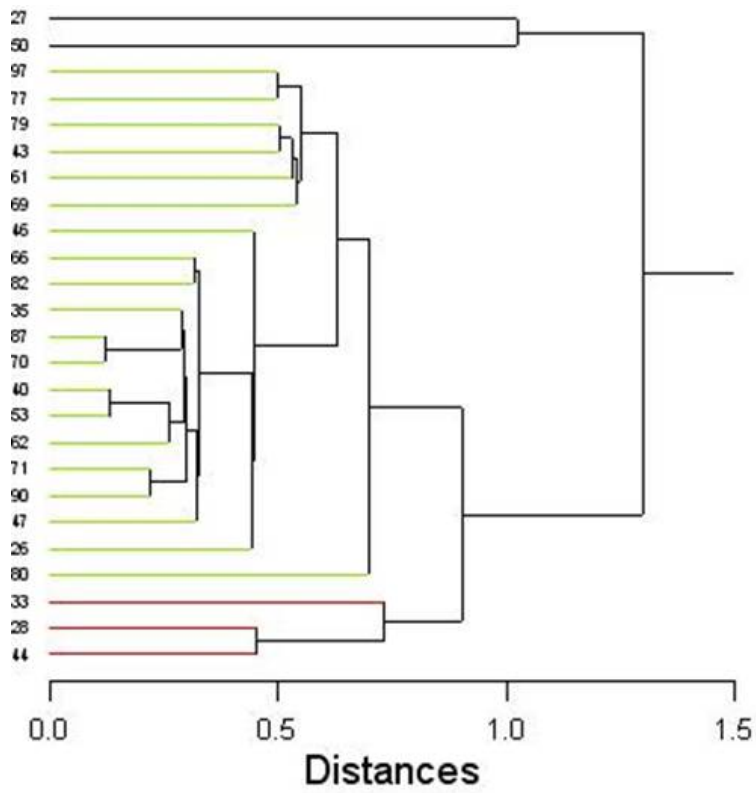


Figure 26. Cluster analysis dendograms of principal components (4: top; 5: bottom) based on BC spectra

The number of differences between the PCA of NBC and BC spectra, however, was larger. Sample 27 was not clustered with other samples based on NBC spectra normalized using the first method however when baseline correcting sample 27 was grouped with sample 50 as the most distinctly separated from the other samples. The larger amount of smaller groupings found in the cluster analysis based on the NBC spectra is not found in the analysis based on the BC spectra.

Peak Analysis

Sorenson

Spectra were simultaneously baseline corrected while the peaks were identified.<sup>55</sup> The Sorenson index was calculated (Eqn. 7) for comparisons between spectra and the samples were compared using a two-tailed t-test based on the indices. The results of the discrimination from different sample sets can be seen in Table 8.

Table 8. Sorenson/t-test discrimination percentages based on drill down spectra

	Different Sample Comparison (%)	Same Sample Comparison (%)
8 <sub>1</sub> v 8 <sub>2</sub>	50.9	20.0
8 <sub>1</sub> v 9 <sub>25</sub>	65.3	75.0
8 <sub>2</sub> v 9 <sub>25</sub>	60.0	70.8
9 v 9	78.4	

Data sets 8<sub>1</sub>, 8<sub>2</sub> and 9<sub>25</sub> came from spectra from the same samples. Spectra for data sets 8<sub>1</sub> and 8<sub>2</sub> (Appendix: Drill Down, Experiment 8) were taken on the same day with data set 8<sub>1</sub> originating from the first set of chips from each sample and 8<sub>2</sub> being

derived from the second set of chips from each sample. Data set 9<sub>25</sub> was taken a month later and is a part of the larger group of samples from Experiment 9 (Appendix: Drill Down). The Sorenson indices for different sample comparisons ranged from 0.09 to 0.992 while those for same sample comparisons ranged from 0.09 to 0.825.

The comparisons between sample sets collected on the same day yielded the lowest discrimination between different samples but also had the lowest same sample discrimination. As the discrimination increased for comparisons of data sets from different days, the same sample discrimination also increased.

#### MANOVA/ANOVA/Tukey

Fifty-two wavelengths were chosen based on peaks that were common in five representative baseline corrected spectra from LIBS Drill Down, Experiment 8. However, only twenty of the twenty-five samples analyzed during Experiment 8 were used for this data analysis and are indicated under Experiment 8a in the Appendix. The intensities of these 52 wavelengths were extracted from the baseline corrected spectra and ordered into a data set for analysis by the Statistical Analysis System (SAS) software. MANOVA was performed on the data set to determine whether there was a significant difference between the intensities at different wavelengths and, if so, between the samples based on the emission intensities at each wavelength (ANOVA and Tukey).

The Wilks' lambda for the MANOVA was 0.00 while the p-value was <.001. This result indicates that there was a difference between the emissions at different wavelengths in at least two of the wavelengths when they were compared simultaneously across all samples. This meant that the subsequent ANOVA for each wavelength could be analyzed. Each ANOVA for each wavelength had a p-value of <.001 which indicated

that the null hypothesis could be rejected and it could be concluded that there was a significant difference between at least two of the samples with respect to each wavelength. It also signified that the Tukey HSD test results could be interpreted. The Tukey HSD test was able to discriminate between samples based on the wavelength.

Based on the results from the Tukey HSD tests, discrimination matrices could be constructed for each wavelength (Table 9). The samples 1 and 21, 2 and 22, etc., were different chips from the same sample. The comparisons indicated with a “1” signify that the comparison was discriminated while the comparisons with a “0” indicated that the comparison was not discriminated. The matrix is symmetrical about the diagonal. For this wavelength, the discrimination between different sample comparisons was only 24.9%, but importantly none of the same sample comparisons were discriminated against each other.

Table 9. Tukey discrimination matrix for Wavelength 1 (394.43 nm).

	1	2	3	4	5	6	7	8	9	10	11	12	13	14	15	16	17	18	19	20	21	22	23	24	25	26	27	28	29	30	31	32	33	34	35	36	37	38	39	40														
1	0																																																					
2	0	0																																																				
3	0	0	0																																																			
4	0	0	0	1																																																		
5	1	1	1	0	0																																																	
6	0	0	1	0	0	0																																																
7	0	0	1	0	0	0	0																																															
8	0	0	0	0	1	1	1	1																																														
9	0	0	0	1	1	1	1	1	0																																													
10	0	0	1	0	0	0	0	1	1	0																																												
11	0	0	1	0	0	0	0	1	1	0	0																																											
12	0	0	1	0	0	0	0	1	1	0	0	0																																										
13	0	0	1	0	0	0	0	1	1	0	0	0	0																																									
14	1	0	1	0	0	0	0	1	1	0	0	0	0	0																																								
15	0	0	1	0	0	0	0	1	1	0	0	0	0	0	0																																							
16	1	1	1	0	0	0	0	1	1	0	0	0	0	0	0	0																																						
17	0	0	1	0	0	0	0	1	1	0	0	0	0	0	0	0	0																																					
18	0	0	1	0	0	0	0	1	1	0	0	0	0	0	0	0	0	0																																				
19	1	0	1	0	0	0	0	1	1	0	0	0	0	0	0	0	0	0	0																																			
20	0	0	1	0	0	0	0	1	1	0	0	0	0	0	0	0	0	0	0	0																																		
21	0	0	0	0	1	0	0	0	0	0	0	0	0	1	0	1	0	0	0	1	0	0																																
22	0	0	1	0	0	0	0	1	0	0	0	0	0	0	0	0	0	0	0	0	0	0	0																															
23	0	0	0	1	1	1	1	0	0	1	1	1	1	1	1	1	1	1	1	1	1	1	0	0																														
24	0	0	1	0	0	0	0	1	1	0	0	0	0	0	0	0	0	0	0	0	0	0	0	0	1	0																												
25	1	1	1	0	0	0	0	1	1	0	0	0	0	0	0	0	0	0	0	0	0	1	0	1	0	0																												
26	0	0	1	0	0	0	0	1	1	0	0	0	0	0	0	0	0	0	0	0	0	0	0	1	0	0	0																											
27	0	0	1	0	0	0	0	1	1	0	0	0	0	0	0	0	0	0	0	0	0	0	0	1	0	0	0	0																										
28	0	0	0	1	1	1	1	0	0	1	1	1	1	1	1	1	1	1	1	1	1	0	0	0	0	1	1	1	0																									
29	0	0	0	0	1	1	1	0	0	1	1	1	1	1	1	1	1	1	1	1	1	0	0	0	0	1	1	1	0	0																								
30	0	0	1	0	0	0	0	1	1	0	0	0	0	0	0	0	0	0	0	0	0	0	0	1	0	0	0	0	0	1	1	0																						
31	0	0	1	0	0	0	0	1	1	0	0	0	0	0	0	0	0	0	0	0	0	0	0	1	0	0	0	0	0	1	1	0	0																					
32	0	0	1	0	0	0	0	1	1	0	0	0	0	0	0	0	0	0	0	0	0	0	0	1	0	0	0	0	0	1	1	0	0	0																				
33	0	0	1	0	0	0	0	1	1	0	0	0	0	0	0	0	0	0	0	0	0	0	0	1	0	0	0	0	0	1	1	0	0	0	0																			
34	0	0	1	0	0	0	0	1	1	0	0	0	0	0	0	0	0	0	0	0	0	0	0	1	0	0	0	0	0	1	1	0	0	0	0	0																		
35	1	0	1	0	0	0	0	1	1	0	0	0	0	0	0	0	0	0	0	0	0	1	0	1	0	0	0	0	1	1	0	0	0	0	0	0	0																	
36	0	0	1	0	0	0	0	1	1	0	0	0	0	0	0	0	0	0	0	0	0	0	0	1	0	0	0	0	1	1	0	0	0	0	0	0	0	0	0															
37	0	0	1	0	0	0	0	1	1	0	0	0	0	0	0	0	0	0	0	0	0	0	0	1	0	0	0	0	1	1	0	0	0	0	0	0	0	0	0	0	0	0	0	0	0	0	0	0	0					
38	0	0	1	0	0	0	0	1	1	0	0	0	0	0	0	0	0	0	0	0	0	0	0	1	0	0	0	0	1	1	0	0	0	0	0	0	0	0	0	0	0	0	0	0	0	0	0	0	0	0				
39	0	0	1	0	0	0	0	1	1	0	0	0	0	0	0	0	0	0	0	0	0	0	0	1	0	0	0	0	1	1	0	0	0	0	0	0	0	0	0	0	0	0	0	0	0	0	0	0	0	0	0			
40	0	0	1	0	0	0	0	1	1	0	0	0	0	0	0	0	0	0	0	0	0	0	0	1	0	0	0	0	1	1	0	0	0	0	0	0	0	0	0	0	0	0	0	0	0	0	0	0	0	0	0	0		

The F values obtained from each ANOVA indicated the relative strength of each wavelength's discrimination although it was not absolute (i.e. the wavelength with the highest F value did not have the highest discrimination over all wavelengths). Each discrimination matrix for each wavelength was combined with others by establishing that discrimination of one comparison by one wavelength meant that the samples were discriminated regardless of the result from other wavelengths.

Fourteen wavelengths were identified that were able to discriminate the largest number of different sample comparisons while limiting the number of discriminated same sample comparisons to a minimum. The discrimination matrix (Table 10) displays the result of combining the discriminations from these wavelengths in which sample comparisons were considered discriminated based on discrimination in any of the wavelength discrimination matrices. Again, sample 1 and 21, 2 and 22, 11 and 31, etc., are from the same sample but from different chips. As seen in other discrimination matrices, 1 indicates discrimination between the compared samples while 0 indicates that the samples were not discriminated. A discrimination of 87.5% for different sample comparisons was found while the same sample discrimination was limited to 1 in 20 (5%).





The fourteen wavelengths that were used for this discrimination (Table 11) were “identified” using both the OOILIBS software as well as a standard reference.<sup>66</sup> While occasionally the software and MIT wavelength tables agree on certain wavelengths (WL 1, 7, 15, 21 and 41), the assignments from the MIT wavelength tables are more reliable.

Table 11. Wavelengths used for MANOVA, their possible elemental identification and discrimination

Wavelength (nm)	Source		Discrimination of Samples (%)
	OOILIBS Software	MIT Wavelength Tables	
WL 1 394.43	Al	Al	24.9
WL 3 453.60	NA	Ti	47.1
WL 6 514.67	NA	Co	55.1
WL 7 517.31	Mg	Mg	61.4
WL 8 519.23	NA	NA	63.8
WL 10 522.34	NA	Ti	43.3
WL 15 553.51	Ba	Ba	43.8
WL 16 566.16	NA	Ti	55.3
WL 20 586.57	NA	Ti	55.5
WL 21 588.91	Na	Na	19.7
WL 24 599.67	NA	Ni	53.1
WL 28 614.09	NA	Ba	38.3
WL 30 626.04	NA	Ti	47.2
WL 41 670.70	Li	Li	33.5

NA: Not assigned

## Discussion

The drill down approach has provided certain challenges during the experimental and subsequent data analysis. The shape of the crater formed by the ablation of the sample may be attributed to several factors. The beam energy profile for the laser used during this research should have been Gaussian but did not appear to be. The interaction between the laser and the sample (i.e. melting and ejecting of matter) may have caused

areas outside the main irradiance area to be ablated although the directionality of the ablation did not support this. Since the profile did not appear to be Gaussian, the upper layers from one of the sides of the crater may have contributed to the subsequent spectra. These problems affected the spectra and, therefore, the analysis of the spectra.

It has been reported previously that drilling down through the layers has not been the optimum method for examining layers due to fluctuations in the laser<sup>31</sup> and the laser profile. This was found to be a problem in this research when attempting to differentiate between the layers. Correlations between spectra from the same drill down remained relatively high in most samples so that differentiating between the layers was not possible.

Several varieties of data analysis for LIBS drill down spectra have been explored. While the full spectrum analysis was more convenient to utilize (no need of baseline correcting and finding peaks), the peak analysis (i.e. MANOVA, etc.) offered specificity and elimination of the many baseline points which could incorrectly influence the data analysis leading to Type I and Type II errors. However, this tendency did not appear to be relevant in the results. Results from the full spectrum data analysis appeared to give higher different sample discrimination than the peak analysis (Z(r)/t-test: 99.7%) while for peak analysis lower same sample discrimination could be achieved (MANOVA: 5%).

The library method based on HQI values produced an area under the ROC curve that was extremely high and approached ideal behavior. The dot histogram also showed that the same sample HQI values also tended to gather near the abscissa which was not observed during analysis of cross section spectra. The relative success of this method suggests that limiting the number of pulses per averaged spectrum for each sample might be advantageous, regardless of chip thickness.

Averaging of the drill down spectra during experiments both on substrate and isobutylene appeared to improve the results. However, in some cases discrimination between points on the same sample (i.e. high same sample discrimination) was achieved which is not desirable (see Table 12). Baseline correcting the spectra improved both the different sample discrimination as well as lowered the same sample discrimination. Samples that were not discriminated could be linked by similar manufacturer, color and/or year for the HQI or Z(r) with t-test analyses. However, high discrimination between same sample comparisons of spectra taken on separate days still occurred even when the spectra were baseline corrected.

Table 12. Review of results from data analysis of drill down spectra

Data Analysis	Error (%)	
	Type I	Type II
HQI Library	10.0	0.4
HQI/t-test	12.5 – 16.0	0.6 – 5.5
Z(r)/t-test	12.0 – 20.0	0.3 – 4.7
Sorenson/t-test	20.0 – 75.0	21.6 - 49.1
MANOVA	5.0	12.0

For the PCA/cluster analysis based on NBC spectra, while the number of significant eigenvalues that were chosen was usually greater than one, the first eigenvalues contained at least 90% of the variance for each analysis. When visually inspecting the NBC spectra normalized by the first method (Figure 27), it appeared that the baseline was accounting for the largest variance. The spectrum at the bottom had a relatively small baseline in comparison to the spectrum that is second from the top which had a larger baseline. This effect was also found when the spectra were normalized by the second method although the effect was not as pronounced.

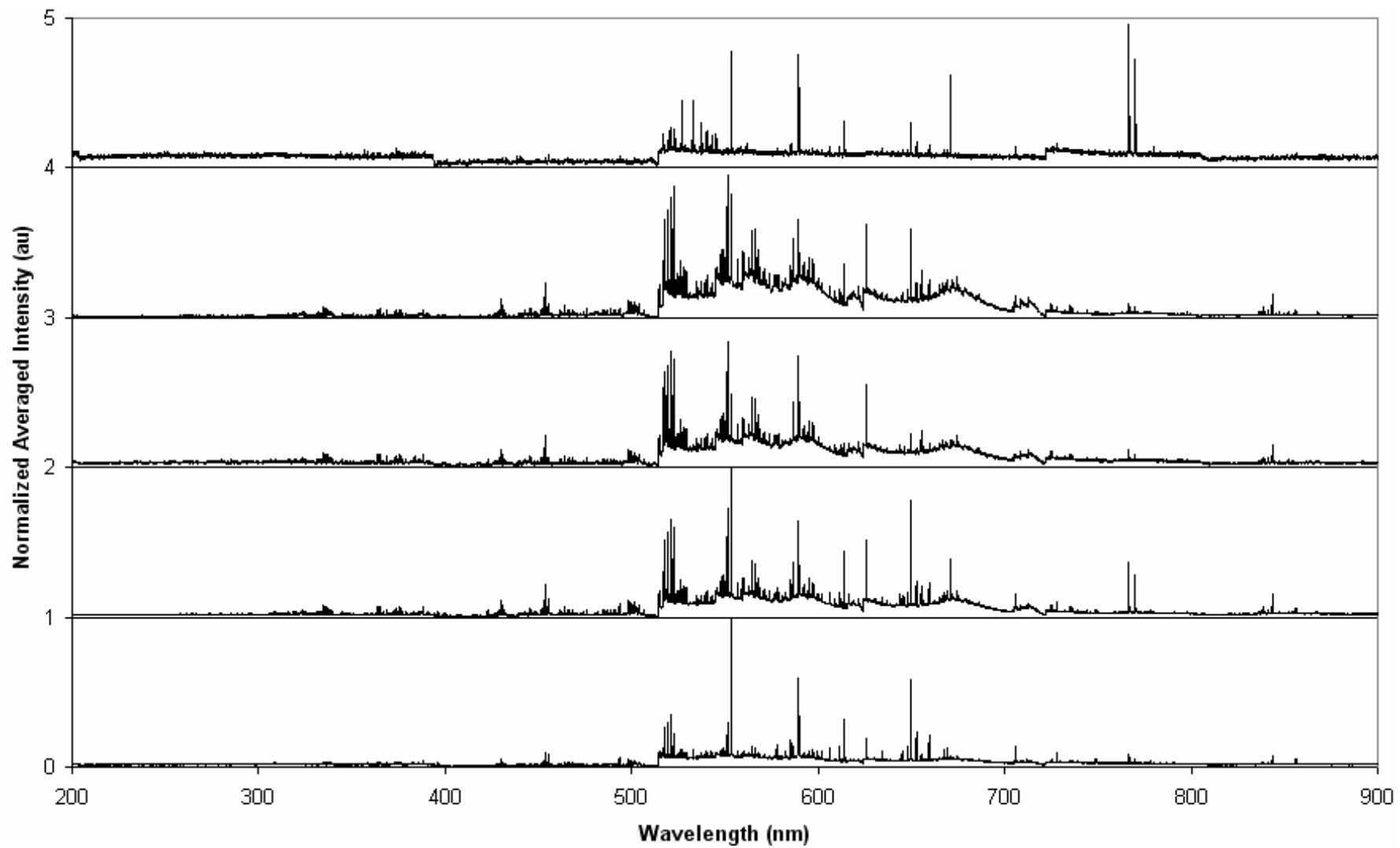


Figure 27. Representative averaged spectra from PCA/cluster data analysis

When the baseline was corrected, physically meaningful groupings were not found. The number of groupings decreased so that there were three small groups of one or two samples each and one very large group suggesting that all of the samples are very similar and could not be discriminated using this method. Limiting the range of wavelengths used for the analysis might be prudent so that the analysis is focused on a limited number of peaks.

The MANOVA and subsequent analyses produced relatively high different sample discrimination and lower same sample discrimination than full spectrum data analysis methods. However, the complexity of the procedure makes it intimidating and time consuming. While the wavelengths were identified with elements, the identifications were not certain due to the resolution of the spectrometers.

The variety of different data analyses allowed for an overall assessment of the LIBS Drill Down experiments. Reproducibility continued to be a problem while discrimination between the full spectrum of a large amount of samples (up to 93) was very high.

## CHAPTER 5: SEM/EDS & FTIR-ATR

### SEM-EDS

The cross sections of twenty-six samples were analyzed with the SEM/EDS. The sampling area for each spectrum encompassed all layers of the cross section and three spectra per sample were collected. Figure 28 shows a typical spectrum from an automotive paint sample. Several different elements can be observed including carbon, iron, titanium, magnesium and aluminum which were identified with the aid of instrument manufactured software.

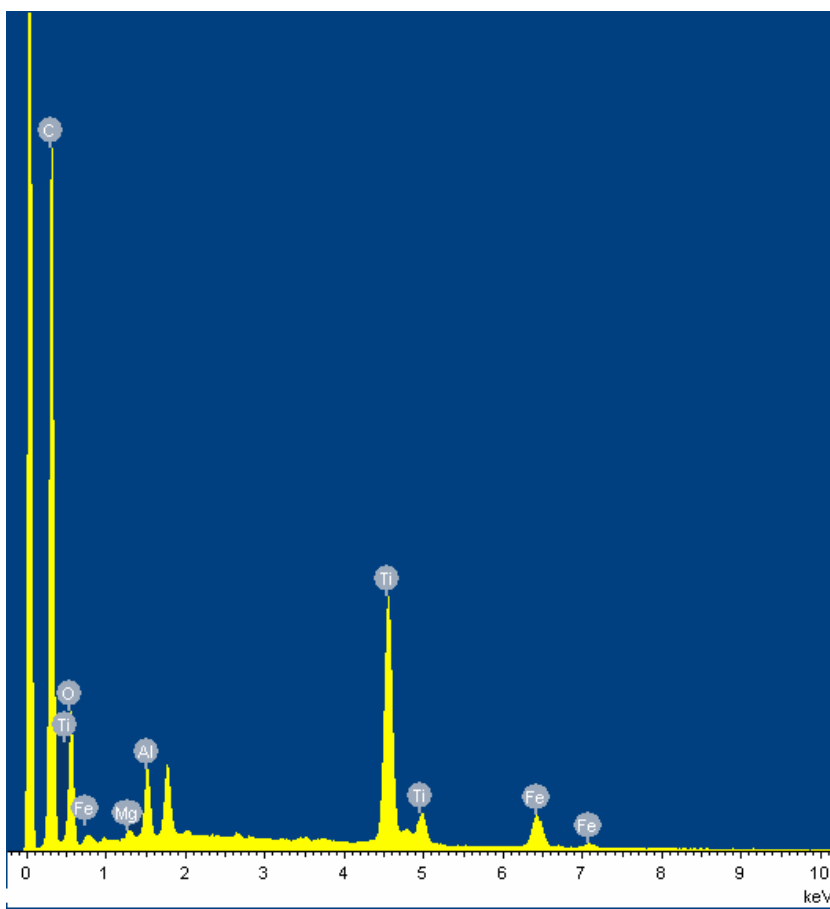


Figure 28. EDS spectrum of Pontiac GTO

## Results

Using the HQI, Z(r) and the Sorenson index values as bases for t-tests, the samples were compared. The results from the different sample comparisons (Table 13) show discrimination as high as 70.6% from the baseline corrected spectra comparisons using HQI. The Sorenson index based t-tests discriminated only 37.8% of the samples.

Table 13. T-test results from SEM/EDS analysis

	HQI	Z(r)	Sorenson
Non-Baseline Corrected	70.4	69.0	
Baseline Corrected	70.6	69.3	37.8

## FTIR-ATR

A sample spectrum from the analysis can be seen in Figure 29. At  $1452\text{ cm}^{-1}$  there is C-H bending with corresponding C-H stretching  $2800\text{-}2960\text{ cm}^{-1}$ . The peaks around  $1700\text{ cm}^{-1}$  indicate the presence of a carbonyl while the stretching bands between  $1000$  and  $1175\text{ cm}^{-1}$  imply that the carbonyl might be part of an ester group. According to the classification developed by Ryland<sup>67</sup>, this sample's clearcoat is possibly an alkyd (alcohol + acid).



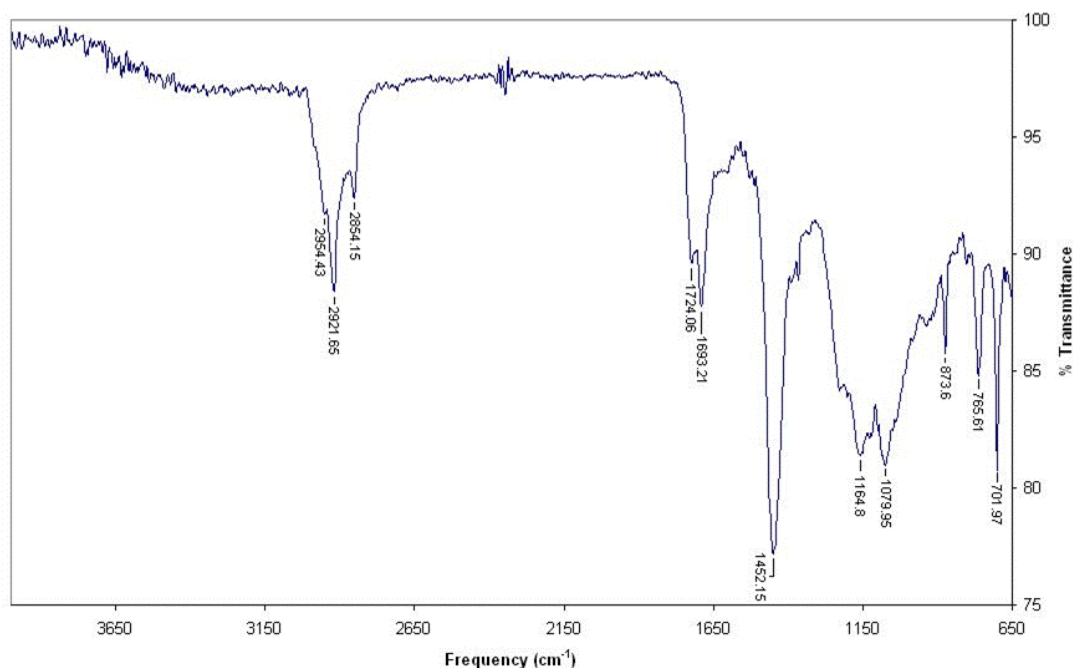


Figure 29. FTIR-ATR transmittance spectrum of the clearcoat of 2005 Pontiac GTO

## Results

The results from the HQI/t-test analysis can be seen in Table 14 which has been arranged according to groups which contain samples that are discriminated or not discriminated from similar samples (for example, group A is not discriminated from themselves, group B and C). The discrimination matrix is symmetric about the diagonal (highlighted in yellow) and “1” indicates the samples were discriminated while “0” indicates that the samples were not discriminated.

Each of the five groups (A, B, C, D and E) contains a similar number of samples except for E which only contains Sample 37 which was discriminated from all other samples due to large absorption bands at  $634\text{ cm}^{-1}$  and below. For groups A, C and D the



samples within the group are not discriminated from each other for the most part.

According to the classification determined by Ryland, group A contained acrylic melamine, group C mainly acrylic urethanes and group D was made up of spectra from samples which were devoid of strong absorption bands (i.e. poor spectra).

The same was not found for the samples within group B. For this reason, group B was a mixture of samples that did not fit in the remaining groups but were not necessarily discriminated from themselves. The group was made up of samples of possible alkyd and/or acrylic melamine (as seen by nondiscrimination between samples in group A and B). The groups determined by the HQI/t-tests were the same as those determined by the Z(r)/t-tests.

Discrimination between different sample comparisons reached 62.7% based on HQI/t-tests. When the Z(r) values were compared using the t-test, the discrimination dropped slightly to 62.1%.

Table 15. Combination of results from SEM/EDS and FTIR-ATR analyses

HQI		FTIR-ATR	SEM/EDS	
			NBC	BC
FTIR-ATR		62.7		
SEM/EDS	NBC	88.0	70.4	
	BC	88.0		70.6

Z(r)		FTIR-ATR	SEM/EDS	
			NBC	BC
FTIR-ATR		62.1		
SEM/EDS	NBC	88.0	69.0	
	BC	87.0		69.3

When combining the results for the thirteen samples that were analyzed by both SEM/EDS and FTIR-ATR, the discrimination increased to 88% (Table 15). There was very little difference between the different metrics used for the subsequent t-test and also between the spectra that were baseline corrected with those that were not.

## Discussion

Between the SEM/EDS and FTIR-ATR analyses, the SEM/EDS appeared to better discriminate between the samples. This could be due to differences in the experimental analysis of the samples between the two instruments. Using the FTIR-ATR, the analysis was limited to the clearcoat. During SEM/EDS analysis, the entire cross section was interrogated although the SEM/EDS analysis only addressed the inorganic components within the layers which limited the analysis to the pretreatment, electrocoat, surfacer and possibly the basecoat.

The low discrimination from the Sorenson index based t-tests is due in part to the fact that many of the samples shared the same peaks, i.e. elements. This was not unexpected since certain elements are relatively common in most layers of automotive paint, for example, titanium, aluminum and iron. The calculated HQI or  $Z(r)$  were more precise than the Sorenson index since they take into account all points of the spectrum while the Sorenson index is only concerned with the peaks. The HQI and  $Z(r)$  values provided higher discrimination during the t-test between different sample comparisons.

As has been reported elsewhere<sup>29, 30</sup> when combining the results from the two instrumental analyses, higher discrimination between the different sample comparisons was found relative to both analyses by themselves. Higher discrimination that was typically found using the HQI values in comparison with the  $Z(r)$  values in previous data

analyses was not found when the two analyses results were combined. However, the samples that were not discriminated were not similar in their physical characteristics, for example, color, presence of effect pigments, number of layers, etc.

## CHAPTER 6: CONCLUSIONS AND FUTURE RESEARCH

### Conclusions

Obtaining reproducible LIBS spectra from the cross section appeared to be very difficult due to a variety of factors. The different sample discrimination between the cross section spectra was high; however, the impact of this result was nullified by the high same sample discrimination. Increasing the number of spectra and averaging them did not create a better result.

Averaging the spectra from the drill down analysis, however, was the best method for obtaining optimal discrimination results from LIBS spectra. The drill down approach produced more reproducible spectra than the cross section yielding lower same sample discrimination than the cross section analysis. The areas under the curve from the ROC analyses based on the Library analyses of the cross section and drill down spectra were in agreement with this assessment.

However, reproducibility was still a problem for the LIBS drill down spectra. Baseline correcting the spectra in conjunction with the  $Z(r)$  based t-test improved the same sample discrimination. However, the same sample discrimination could only be reduced to 12.0%. Using the MANOVA analysis, the same sample discrimination was limited to one in twenty samples.

The different sample discrimination from the FTIR-ATR and SEM/EDS individually was much lower than those from the LIBS analyses; however, the reproducibility problems found in the LIBS spectra have been proven to be a much smaller problem with FTIR and SEM/EDS instruments. Even when the results from

these two instruments were combined, the different sample discrimination was still not quite as high as that from LIBS.

## Future Research

### Automotive Paint

In the future, perhaps a better way of analyzing paint samples as well as other “softer” materials would be to use a femtosecond laser as opposed to the nanosecond laser used in the LIBS experiments reported here. Baudelet, et al demonstrated the positive outcome of using such a laser on biological samples.<sup>32</sup> These included lower (practically negligible emission from excited ambient air) and faster decreasing plasma temperature and explosive ejection of matter, and molecular spectral signatures of a sample together with the atomic emissions. Cravetchi, et al also evaluated femtosecond lasers used in LIBS experiments, and compared the results to those from nanosecond lasers.<sup>68</sup> The results were similar.

A possible solution to the focusing problem found in the cross section analysis might be to use a microscope to focus the laser. Gornushkin, et al, have described and used a microscope setup for analysis of solid materials.<sup>69</sup> A crater diameter of ~20  $\mu\text{m}$  was achieved at a working distance of 5 mm for a 10x objective. The diameter was similar to the width of individual automotive paint layers.

### LIBS

As Locard has stated<sup>70</sup>, “physical evidence cannot be wrong, it cannot perjure itself, it cannot be wholly absent. Only human failure to find it, study and understand it, can diminish its value.” The understanding of the results from any chemical experiment

is perhaps the most important part in determining results and conclusions. It is therefore imperative that it is understood what happens when a sample is interrogated with a laser. Continued work on understanding the processes and what affects those processes during a LIBS experiment will help to interpret results and provide a better understanding of how to proceed towards making LIBS a better method for analyzing samples especially complex matrices such as automotive paint chips.

Control of the sampling atmosphere might also be a factor in obtaining more reproducible data. The sample chamber used during this research was not airtight and so could not be evacuated or completely filled with an inert gas (e.g. He, Ar). An inert gas would not contribute to the spectra as air does since it does not interact with elements found within the sample. Evacuating the chamber might also give a cleaner spectrum because there is less interference between the plasma and collecting lens.<sup>31</sup>

Another method for dealing with the atmosphere of a sample chamber that is not airtight is to use double pulse LIBS.<sup>71</sup> Two pulses of a laser which are microseconds apart are shot at a sample either normal or parallel to each other. When the pulses are parallel to each other, the first laser pulse creates a vacuum and the second creates the plasma. This setup has resulted in an increase of signal and decreased introduction of atoms from the atmosphere (N, O, etc.). However, since more laser pulses are used, more of the sample is ablated.

#### Distribution free analysis

These types of analyses are also referred to as non-parametric data analyses.<sup>72</sup> These methods have the drawbacks of producing results that are difficult to relate to the real world and may contain severe computational difficulties, and these methods are



relatively new so they are not as well established as other methods. Their power is also not as great as parametric tests. Samples that might be discriminated using a parametric test might not necessarily be so using a non-parametric test. There are some routes around the computational problems by simplifying and estimating. However, using this type of analysis is statistically more rigorous than altogether ignoring the necessity of a normal distribution.

The name distribution-free is misleading since it suggests that there is not a distribution involved in the analysis. There is no assumed distribution before analysis of the data (for example, the decomposition found in PCA). A model is formed based on the data and not vice versa. Several different tests have been developed including those specifically categorizing data as non-Gaussian.

For example, a parametric measurement such as Pearson's correlation has nonparametric equivalents in Spearman's rank correlation and Kendall's tau. As opposed to calculating the value without altering the data as is done with Pearson's correlation, the data is ranked prior to calculation of the value. Spearman's rank correlation uses the same equation as the Pearson's correlation (Eqn. 3) while Kendall's tau ( $t_k$ ) is calculated using the following equation.

$$t_k = \frac{n_c - n_d}{\frac{1}{2}n(n-1)}$$

$n_c$  is the number of concordances between two spectra based on their ranked data while  $n_d$  is the number of discordances. Using rank is a form of permutation which along with randomization forms the basis for nonparametric statistical tests.<sup>73</sup>

## Combination Plots

In an attempt to apply a distribution free statistical analysis, the two sets of spectra generated from twenty of the twenty-five samples from LIBS Drill Down, Experiment 8 were used for this data analysis. The twenty samples whose spectra were used are indicated in the column Experiment 8a (Appendix). Three separate distances were calculated between the spectra which included Euclidean,  $\sin^2\theta$ , and  $1-r$  where  $r$  is the Pearson correlation coefficient. These were used to construct plots (Figure 30) in order to differentiate between samples based on all three distances.<sup>74</sup> Individual refers to the individual distances calculated between spectra, while average indicates the average distances calculated between samples.

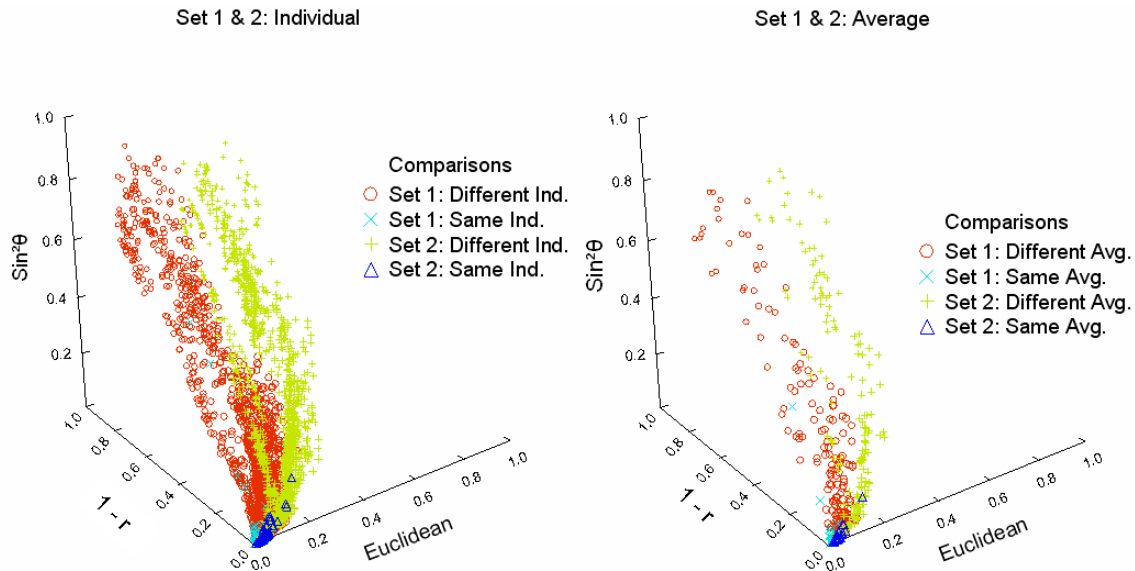


Figure 30. Combination plots using three calculated values

Distances between spectra from the same sample are located close to the origin (0,0,0), while distances between spectra from different samples appear to follow a curve

due to the relationship between the Euclidean distance and  $\sin^2\theta$  values. From these plots, confidence volumes were established based on the values for the same sample distances. The maximum values from the same sample comparisons for each calculated metric established the limit of the confidence volume. The different sample comparisons outside of the volume were characterized as discriminated (Table 16).

The discrimination based on the established volumes reaches 95.8 % when averages of the distances and only 95 % of same sample comparisons were used. This number drops to 76.8% when all the averages of same sample comparisons are used to construct the confidence volume.

Table 16. Percent discrimination of different comparisons outside of the confidence volume

Using all same sample comparisons

	Set 1	Set 2
Individual	48.25	70.41
Average	72.11	76.84

Using 95% of same sample comparisons

	Set 1	Set 2
Individual	78.83	90.12
Average	89.47	95.79

While the combination plots attempted to address possibly non-Gaussian data and provide a method to analyze it, the resulting discrimination was low in comparison to other statistical methods used to analyze drill down spectra. Again, the reproducibility, as with other data analyses, from Set 1 to Set 2 was poor, as can be seen in Figure 29. The 1-r values appeared to define the distinction between values from Set 2 (green +) which were closer to the Euclidean axis (1-r values were lower) than the values from Set 1 (red O) (1-r values were higher). However, the relative position between the respective

calculated distances within each set was similar. This suggests that between sets of data, calculated values (Euclidean distance, etc.) changed but relative placement of comparisons within the sets did not change from set to set.

Currently other nonparametric methods are being attempted such as permutations in order to investigate the number of spectra needed to encompass the variability within the LIBS instrumental analysis. This research will lead to a decrease in the Type I error that parametric methods have not been able to reduce.

## APPENDIX

Number	Year	Manufacturer	Make	Color	Effect Pigment	Substrate	Layers	Experiment										
								LIBS Cross Section			LIBS Drill Down				FTIR-ATR		SEM/EDS	
								1	2	3,4,5,6	7	8	8a	9	CC			
1	2004	Chevrolet	Impala	white	no	plastic	2	✓	✓		✓						M	
2	2003	Dodge	Neon	yellow	no	plastic and chip	5	✓	✓	✓	✓			✓			M	✓
3	2001	Ford	F-series	white	no	plastic	3	✓	✓		✓						M	
4	2002	Ford	Focus	gold	yes	plastic	2	✓	✓		✓						L	
5	2002	Ford	Mustang	grey	yes	plastic	2	✓	✓		✓			✓			U	
6	2003	Ford	Explorer	grey	yes	metal	4	✓	✓		✓			✓			M	
7	2003	Honda	CRV	white	no	metal	4	✓	✓		✓			✓			L	
8	2004	Honda	Civic	red	no	plastic	2	✓	✓		✓			✓			U	
9	2006	Kia	Sportage	grey	yes	plastic	3	✓	✓		✓			✓			U	
10	1998	Mazda	626	red	yes	plastic	3	✓	✓		✓			✓			U	
11	2004	Nissan	Frontier	red	no	plastic	1	✓	✓		✓			✓			M	
12	2004	Nissan	Infiniti G35	grey	yes	plastic	1	✓	✓		✓			✓			L	
13	2004	Nissan	Pathfinder	silver	yes	chip	6	✓	✓		✓			✓			U	✓
14	2004	Nissan	Quest	Lt. blue	yes	plastic	2	✓	✓		✓			✓			M	
15	2005	Nissan	Altima	black	yes	plastic	1	✓	✓		✓			✓			U	
16	1997	Oldsmobile	Regency	white	no	plastic	3	✓	✓		✓			✓			U	
17	2003	Pontiac	Grand Am	grey	yes	plastic	2	✓	✓		✓			✓			U	✓
18	2005	Pontiac	GTO	red	no	chip	8	✓	✓		✓			✓			A	✓
19	2003	Saturn	Ion	grey	yes	plastic	3	✓	✓		✓			✓			U	
20	2005	Saturn	Ion	white	no	plastic	2	✓	✓		✓			✓			U	
21	2005	Subaru	Outback	black	yes	metal	3	✓	✓		✓			✓			M	
22	1991	Toyota	MR2	grey	yes	plastic	2	✓	✓		✓			✓			U	
23	2003	Toyota	4Runner	grey	yes	metal	4	✓	✓		✓			✓			A	
24	2004	Toyota	Scion xB	grey	yes	plastic	2	✓	✓		✓			✓			U	
25	2003	Volkswagon	Passat	grey	yes	metal	3	✓	✓		✓			✓			U	
26	2004	Dodge	Caravan	silver	yes	metal	7		✓				✓	✓			L	
27	1995	Chevrolet	S-10	red	yes	metal	3		✓				✓	✓			U	
28	1989	Chrysler	New Yorker	black	no	metal	5		✓				✓	✓			L	✓
29	2004	Ford	Ranger Edge	blue	yes	metal	4		✓	✓			✓	✓			*L	✓
30	1985	BMW	285i	black	yes	metal	9		✓				✓	✓			*	
31	1987	Toyota	Std. 1/2 ton	cream	no	metal	9		✓				✓	✓			*	
32	1996	Ford	Explorer	red	yes	metal	4		✓	✓			✓	✓			M	✓
33	1987	Dodge	Ram	blue	yes	metal	4		✓				✓	✓			*L	✓
34	1999	Saab	9-3 S	green	yes	metal	3		✓				✓	✓			*	✓

CC: Clearcoat assignment according to Ryland; M: acrylic melamine; L: acrylic lacquer; U: acrylic urethane; A: alkyd; \*: unassigned.

Number	Year	Manufacturer	Make	Color	Effect Pigment	Substrate	Layers	Experiment										
								LIBS Cross Section			LIBS Drill Down				FTIR-ATR		SEM/EDS	
								1	2	3,4,5,6	7	8	8a	9	CC			
35	1988	BMW	325i	gold	yes	metal	3		√				√	√	√	√	L	
36	2001	Volkswagon	Golf	pink	no	plastic	2		√									
37	2000	Toyota	Tacoma	white	no	metal	3		√								*	
38	1995	Honda	Civic	white	no	metal	5		√		√						U	√
39	1999	Ford	Explorer	blue	no	metal	4		√								M	
40	1999	Dodge	Ram	black	no	metal	3		√			√	√				*	
41	1995	GMC	Jimmy	teal	yes	plastic	2		√									
42	1998	Dodge	Caravan	blue	yes	metal	4		√								*	
43	1999	Ford	Taurus	gold	yes	metal	5		√			√	√				*	
44	1995	Ford	Crown Victoria	white	no	metal	3		√			√	√				*	
45	1999	Hyundai	Sonata	black	no	plastic	1		√								L	
46	2002	Kia	Rio	blue	yes	metal	3		√		√	√					M	√
47	2000	Mazda	626	green	yes	metal	4		√			√	√				U	
48	1992	Toyota	Corolla	tan	yes	metal	7		√		√						U	√
49	1997	Nissan	Sentra	red	yes	metal	5		√		√						L	
50	1993	Nissan	Maxima	red	yes	metal	4		√			√					*	
51	1998	Nissan	Altima	white	no	metal	4		√								U	
52	2001	Chrysler	PT Cruiser	silver	yes	metal	4		√		√						M	√
53	2004	Chevrolet	Tahoe	green	yes	metal	5		√			√	√				M	
54	1996	Ford	Mustang	purple	yes	metal	6		√								U	
55	1994	Cadillac	Deville	green	yes	metal	6		√		√						*	
56	1997	Mercury	Grand Marquis	red	yes	plastic	3		√									
57	1994	Chevrolet	Camaro	blue	yes	plastic	4		√								A	
59	1994	Ford	Probe	blue	yes	plastic	2		√								*	
60	1998	Ford	F150 Lariat	black	no	unknown	5											√
61	2003	Acura (Honda)	CL	silver	yes	unknown	4					√	√					
62	2005	Chrysler	Pacifica	silver	yes	unknown	3					√	√					
63	2006	Suzuki	Forenza	silver	yes	unknown	5											√
64	2000	Mazda	MPV	gold	yes	metal	3											√
65	2006	Dodge	Ram	blue	yes	unknown	3											
66	1998	Infiniti (Nissan)	I30	red	yes	metal	5					√	√					√
67	2004	Mitsubishi	Lancer	black	no	unknown	4											
68	2004	Kia	Spectra	bronze	yes	unknown	5											
69	2006	Nissan	Sentra	blue	yes	metal	4					√						

CC: Clearcoat assignment according to Ryland; M: acrylic melamine; L: acrylic lacquer; U: acrylic urethane; A: alkyd; \*: unassigned.

Number	Year	Manufacturer	Make	Color	Effect Pigment	Substrate	Layers	Experiment									
								LIBS Cross Section			LIBS Drill Down				FTIR-ATR CC	SEM/ EDS	
								1	2	3,4,5,6	7	8	8a	9			
35	1988	BMW	325i	gold	yes	metal	3		√			√	√	√	√	L	
36	2001	Volkswagon	Golf	pink	no	plastic	2		√								
37	2000	Toyota	Tacoma	white	no	metal	3		√							*	
38	1995	Honda	Civic	white	no	metal	5		√		√					U	√
39	1999	Ford	Explorer	blue	no	metal	4		√							M	
40	1999	Dodge	Ram	black	no	metal	3		√			√	√			*	
41	1995	GMC	Jimmy	teal	yes	plastic	2		√								
42	1998	Dodge	Caravan	blue	yes	metal	4		√							*	
43	1999	Ford	Taurus	gold	yes	metal	5		√			√	√			*	
44	1995	Ford	Crown Victoria	white	no	metal	3		√			√	√			*	
45	1999	Hyundai	Sonata	black	no	plastic	1		√		√					L	
46	2002	Kia	Rio	blue	yes	metal	3		√		√					M	√
47	2000	Mazda	626	green	yes	metal	4		√			√	√			U	
48	1992	Toyota	Corolla	tan	yes	metal	7		√		√					U	√
49	1997	Nissan	Sentra	red	yes	metal	5		√		√					L	
50	1993	Nissan	Maxima	red	yes	metal	4		√			√				*	
51	1998	Nissan	Altima	white	no	metal	4		√							U	
52	2001	Chrysler	PT Cruiser	silver	yes	metal	4		√		√					AM	√
53	2004	Chevrolet	Tahoe	green	yes	metal	5		√			√				M	
54	1996	Ford	Mustang	purple	yes	metal	6		√							U	
55	1994	Cadillac	Deville	green	yes	metal	6		√		√					*	
56	1997	Mercury	Grand Marquis	red	yes	plastic	3		√								
57	1994	Chevrolet	Camaro	blue	yes	plastic	4		√							A	
59	1994	Ford	Probe	blue	yes	plastic	2		√							*	
60	1998	Ford	F150 Lariat	black	no	unknown	5										√
61	2003	Acura (Honda)	CL	silver	yes	unknown	4					√	√				
62	2005	Chrysler	Pacifica	silver	yes	unknown	3					√	√				
63	2006	Suzuki	Forenza	silver	yes	unknown	5										√
64	2000	Mazda	MPV	gold	yes	metal	3										√
65	2006	Dodge	Ram	blue	yes	unknown	3										
66	1998	Infiniti (Nissan)	I30	red	yes	metal	5					√	√				√
67	2004	Mitsubishi	Lancer	black	no	unknown	4										
68	2004	Kia	Spectra	bronze	yes	unknown	5										
69	2006	Nissan	Sentra	blue	yes	metal	4					√					



Number	Year	Manufacturer	Make	Color	Effect Pigment	Substrate	Layers	Experiment									
								LIBS Cross Section			LIBS Drill Down				FTIR-ATR CC	SEM/ EDS	
								1	2	3,4,5,6	7	8	8a	9			
70	2005	Chevrolet	Tahoe	green	yes	metal	4					✓	✓	✓			
71	1999	Subaru	Legacy	green	yes	unknown	3					✓		✓			✓
72	2006	Scion (Toyota)	tC	dark grey	yes	unknown	4							✓			
73	2003	Mazda	Protégé	green	yes	unknown	4							✓			✓
74	2004	Chevrolet	Classic	white	no	unknown	3							✓			
75	2005	Toyota	Tacoma	red	no	unknown	4							✓			
76	2002	Kia	Optima	blue	yes	unknown	3							✓			✓
77	2004	Pontiac	Sunfire	black	yes	unknown	3					✓		✓			
78	2001	GMC	Safari	gold	yes	unknown	4							✓			✓
79	2002	Buick	Century	gold	yes	unknown	3					✓	✓	✓			
80	2005	Ford	Excursion	white	no	unknown	3					✓	✓	✓			
81	2005	Nissan	Maxima	bronze	yes	unknown	5					✓		✓			✓
82	2004	Dodge	Grand Caravan	white	no	unknown	4							✓			✓
83	2005	Dodge	Stratus	blue	yes	unknown	5							✓			✓
84	1992	Mercedes	300E	silver	yes	unknown	3							✓			
85	2000	Nissan	Xterra	silver	yes	unknown	5							✓			✓
86	1998	Ford	F150 Lariat	red	yes	unknown								✓			
87	2005	Jeep	Liberty	red	no	unknown	5					✓	✓	✓			
88	2003	Mitsubishi	Galant	white	yes	unknown	3							✓			
89	2004	Chevrolet	Cavalier	silver	yes	unknown	3							✓			
90	2005	Mazda	Tribute	blue	yes	metal	3					✓	✓	✓			
91	2002	Mazda	B3000	red	no	metal	4							✓			
92	2002	Oldsmobile	Bravada	white	no	metal	3							✓			
93	2004	Dodge	Dakota	dark grey	yes	unknown	4							✓			
94	2004	Toyota	Tundra	grey	yes	metal	3							✓			
95	2002	Landrover	Discovery II	black	yes	unknown	2							✓			
96	2005	BMW	325i	black	no	unknown	3							✓			
97	2005	Lincoln	Navigator	white	no	unknown	3					✓	✓	✓			
98	2006	GMC	Canyon	black	yes	unknown								✓			
99	2004	Ford	Ranger	white	no	unknown	3							✓			
100	2002	Chrysler	Voyager	red	no	unknown	4							✓			
101	2004	Chevrolet	Silverado	black	yes	unknown	3							✓			
102	2006	Honda	Pilot	red	yes	unknown	3							✓			
103	2004	GMC	Envoy	green	yes	unknown	3							✓			

Number	Year	Manufacturer	Make	Color	Effect Pigment	Substrate	Layers	Experiment									
								LIBS Cross Section			LIBS Drill Down				FTIR-ATR		SEM/
								1	2	3,4,5,6	7	8	8a	9	CC	EDS	
104	2001	Dodge	Dakota	silver	yes	unknown	4							✓			
105	2002	Honda	Accord	blue	yes	unknown	3							✓			
106	2004	Chevrolet	Colorado	red	no	unknown	3							✓			
107	2006	Toyota	4Runner	dark grey	yes	unknown	4							✓			
108	2004	Pontiac	Montana	gold	yes	unknown	5							✓			
109	2004	Chevrolet	Blazer	red	no	unknown	4							✓			
110	2002	Pontiac	Grand Am	red	no	unknown	4							✓			

## REFERENCES

1. Ryland, S. G.; Kopec, R. J., The Evidential Value of Automobile Paint Chips. *Journal of Forensic Sciences* **1978**, 24, (1), 140-147.
2. Gothard, J. A., Evaluation of Automobile Paint Flakes as Evidence. *Journal of Forensic Sciences* **1976**, 21, (3), 636-641.
3. Thornton, J. I., Forensic Paint Examination. In *Forensic Science Handbook*, 2nd ed.; Saferstein, R., Ed. Prentice Hall: Upper Saddle River, NJ, 2002; Vol. 1, pp 429-475.
4. Standard Guide for Forensic Paint Analysis. In 02, E.-. Ed. ASTM International: 2002.
5. Bentley, J., Composition, manufacture and use of paint. In *Forensic Examination of Glass and Paint: Analysis and Interpretation*, Caddy, B., Ed. Taylor and Francis, Inc.: New York, 2001; pp 123-142.
6. Marrion, A. R., *The Chemistry and Physics of Coatings*. 2nd ed.; The Royal Society of Chemistry: Cambridge, UK, 2004.
7. Streitberger, H.-J.; Goldschmidt, A., *BASF Handbook on Basics of Coating Technology*. BASF Coatings AG: Hannover, Germany, 2003.
8. Smith, H. M., *High Performance Pigments*. Wiley-VCH Verlag-BmbH: Weinheim, Germany, 2002.
9. Wonnemann, H., Primer Surfacer. In *Automotive Paints and Coatings*, 2nd ed.; Streitberger, H.-J.; Dossel, K.-F., Eds. Wiley-VCH Verlag GmbH & Co.: Weinham, 2008.
10. Stoye, D., *Paints, Coatings and Solvents*. 1st ed.; VCH Publishers, Inc.: New York, 1993.
11. Streitberger, H.-J., Introduction. In *Automotive Paints and Coatings*, 2nd ed.; Streitberger, H.-J.; Dossel, K.-F., Eds. Wiley-VCH Verlag GmbH & Co.: Weinham, 2008; p 493.
12. Tippett, C. F., The evidential value of the comparison of paint flakes from sources other than vehicles. *Journal of Forensic Science Society* **1968**, 8, (2), 61-65.
13. Stoecklein, W., The role of colour and microscopic techniques for the characterisation of paint fragments. In *Forensic Examination of Glass and Paint: Analysis and Interpretation*, Caddy, B., Ed. Taylor and Francis, Inc.: New York, 2001; pp 123-142.

14. Suzuki, E. M., Infrared spectra of U.S. automobile original topcoats (1974-1989): I. Differentiation and identification based on acrylonitrile and ferrocyanide C.tplbond.N stretching absorptions. *Journal of Forensic Science* **1996**, 41, (3), 376-392.
15. Suzuki, E. M.; Carrabba, M., In situ identification and analysis of automotive paint pigments using line segment excitation Raman spectroscopy: I. inorganic topcoat pigments. *Journal of Forensic Sciences* **2001**, 46, (5), 1053-1069.
16. Suzuki, E. M.; McDermot, M. X., Infrared spectra of U.S. automobile original finishes. II. Extended range FT-IR and XRF analyses inorganic pigments in situ-nickel titanate and chrome titanate. *Journal of Forensic Science* **2006**, 51, (3), 532-547.
17. Flynn, K.; O'Leary, R.; Lennard, C.; Roux, C.; Reedy, B. J., Forensic Applications of Infrared Chemical Imaging: Multi-Layered Paint Chips. *Journal of Forensic Sciences* **2005**, 50, (4), 832-841.
18. McEwen, D. J.; Cheever, G. D., Infrared Microscopic Analysis of Multiple Layers of Automotive Paints. *Journal of Coatings Technology* **1993**, 65, (819), 35-41.
19. Challinor, J. M., Pyrolysis techniques for the characterisation and discrimination of paint. In *Forensic Examination of Glass and Paint: Analysis and Interpretation*, Caddy, B., Ed. Taylor and Francis, Inc.: New York, 2001; pp 165-182.
20. Burns, D. T.; Doolan, K. P., A comparison of pyrolysis-gas chromatography-mass spectrometry and fourier transform infrared spectroscopy for the characterization of automotive paint samples. *Analytica Chimica Acta* **2005**, 539, (1-2), 145-155.
21. Armitage, S.; Saywell, S.; Roux, C.; Lennard, C.; Greenwood, P., The analysis of forensic samples using laser micro-pyrolysis gas chromatography mass spectrometry. *Journal of Forensic Sciences* **2001**, 46, (5), 1043-1052.
22. Stachura, S.; Desiderio, V. J.; Allison, J., Identification of Organic Pigments in Automotive Coatings Using Laser Desorption Mass Spectrometry. *Journal of Forensic Sciences* **2007**, 52, (3), 595-603.
23. Beam, T. L.; Willis, W. V., Analysis Protocol for Discrimination of Automotive Paints by SEM-EDXA Using Beam Alignment by Current Centering. *Journal of Forensic Sciences* **1990**, 35, (5), 1055-1063.
24. Deconinck, I.; Latkoczy, C.; Gunther, D.; Govaert, F.; Vanhaecke, F., Capabilities of laser ablation-inductively coupled plasma mass spectrometry for (trace) element analysis of car paints for forensic purposes. *Journal of Analytical Atomic Spectrometry* **2006**, 21, (9), 899-909.
25. Hobbs, A. L.; Almirall, J. R., Trace elemental analysis of automotive paints by laser ablation-inductively coupled plasma-mass spectrometry (LA-ICP-MS). *Analytical and Bioanalytical Chemistry* **2003**, 376, (8), 1265-1271.

26. Debnath, N. C.; Vaidya, S. A., Application of X-ray diffraction technique for characterization of pigments and control of paints quality. *Progress in Organic Coatings* **2006**, 56, (2-3), 159-168.
27. Nel, P.; Lau, D.; Hay, D.; Wright, N., Non-destructive micro-X-ray diffraction analysis of painted artefacts: Determination of detection limits for the chromium oxide-zinc oxide matrix. *Nuclear Instruments & Methods in Physics Research, Section B: Beam Interactions with Materials and Atoms* **2006**, 251, (2), 489-495.
28. Kanngießer, B.; Malzer, W.; Rodriguez, A. F.; Reiche, I., Three-dimensional micro-XRF investigations of paint layers with a table top setup. *Spectrochimica Acta Part B* **2005**, 60, 41-47.
29. Van der Ven, L. G. J.; Leijzer, R. T. M.; Van den Berg, K. J.; Ganguli, P.; Lagendijk, R., Interactions between basecoats and clearcoats in car refinish systems. *Progress in Organic Coatings* **2007**, 58, 117-121.
30. Zięba-Palus, J.; Borusiewicz, R., Examination of multilayer paint coats by the use of infrared, Raman and XRF spectroscopy for forensic purposes. *Journal of Molecular Structure* **2006**, 792-793, 286-292.
31. Lee, Y.-I.; Song, K.; Sneddon, J., *Laser-Induced Breakdown Spectroscopy*. Nova Science Publishers, Inc.: Huntington, New York, 2000; p 125.
32. Baudalet, M.; Guyon, L.; Yu, J.; Wolf, J.-P.; Amodeo, T.; Fréjafon, E.; Laloi, P., Femtosecond time-resolved laser-induced breakdown spectroscopy for detection and identification of bacteria: A comparison to the nanosecond regime. *Journal of Applied Physics* **2006**, 99, (8), 084701.
33. Miziolek, A. W.; Palleschi, V.; Schechter, I., *Laser-Induced Breakdown Spectroscopy (LIBS) Fundamentals and Applications*. Cambridge University Press: Cambridge, UK, 2006.
34. Cremers, D. A.; Radziemski, L. J., *Handbook of Laser-Induced Breakdown Spectroscopy*. John Wiley & Sons, Ltd.: West Sussex, England, 2006.
35. Portnov, V. N.; Rosenwaks, S.; Bar, I., Emission following laser-induced breakdown spectroscopy of organic compounds in ambient air. *Applied Optics* **2003**, 42, (15), 2835-2842.
36. Kaminska, A.; Sawczak, M.; Komar, K.; Sliwinski, G., Application of the laser ablation for conservation of historical paper documents. *Applied Surface Science* **2007**, 253, (19), 7860-7864.
37. Gaspard, S.; Oujja, M.; Rebollar, E.; Abrusci, C.; Catalina, F.; Castillejo, M., Characterization of cinematographic films by laser induced breakdown spectroscopy. *Spectrochimica Acta Part B* **2007**, 62B, (12), 1612-1617.

38. Mateo, M. P.; Nicolas, G.; Pinon, V.; Yanez, A., Improvements in depth-profiling of thick samples by laser-induced breakdown spectroscopy using linear correlation. *Surface and Interface Analysis* **2006**, 38, (5), 941-948.
39. Gornushkin, I. B.; Mueller, M.; Panne, U.; Winefordner, J. D., Insights into linear and rank correlation for material identification in laser-induced breakdown spectroscopy and other spectral techniques. *Applied Spectroscopy* **2008**, 62, (5), 542-553.
40. Bousquet, B.; Sirven, J.-B.; Canioni, L., Towards quantitative laser-induced breakdown spectroscopy analysis of soil samples. *Spectrochimica Acta Part B* **2007**, 62, (12), 1582-1589.
41. Bridge, C. M.; Powell, J.; Steele, K. L.; Sigman, M. E., Forensic comparative glass analysis by laser-induced breakdown spectroscopy. *Spectrochimica Acta Part B: Atomic Spectroscopy* **2007**, 62, (12), 1419-1425.
42. Rodriguez-Celis, E. M.; Gornushkin, I. B.; Heitmann, U. M.; Almirall, J. R.; Smith, B. W.; Winefordner, J. D.; Omenetto, N., Laser induced breakdown spectroscopy as a tool for discrimination of glass for forensic applications. *Analytical and Bioanalytical Chemistry* **2008**, 391, (5), 1961-1968.
43. Gottfried, J. L.; De Lucia Jr., F. C.; Munson, C. A.; Miziolek, A. W., Standoff detection of chemical and biological threats using laser-induced breakdown spectroscopy. *Applied Spectroscopy* **2008**, 62, (4), 353-363.
44. Lopez-Moreno, C.; Palanco, S.; Laserna, J. J., Stand-off analysis of moving targets using laser-induced breakdown spectroscopy. *Journal of Analytical Atomic Spectrometry* **2007**, 22, (1), 84-87.
45. Taschuk, M. T.; Tsui, Y. Y.; Fedosejevs, R., Detection and mapping of latent fingerprints by laser-induced breakdown spectroscopy. *Applied Spectroscopy* **2007**, 60, (11), 1322-1327.
46. Dockery, C. R.; Goode, S. R., Laser-induced breakdown spectroscopy for the detection of gunshot residues on the hands of a shooter. *Applied Optics* **2003**, 42, (30), 6153-6158.
47. Martin, M. Z.; Labbe, N.; Andre, N.; Harris, R.; Ebinger, M.; Wullschleger, S. D.; Vass, A. A., High resolution applications of laser-induced breakdown spectroscopy for environmental and forensic applications. *Spectrochimica Acta Part B: Atomic Spectroscopy* **2007**, 62, (12), 1426-1432.
48. Borisov, O. V.; Mao, X.; Russo, R. E., Effects of crater development on fractionation and signal intensity during laser ablation inductively coupled plasma mass spectrometry. *Spectrochimica Acta Part B* **2000**, 55, 1693-1704.

49. Outridge, P. M.; Doherty, W.; Gregoire, D. C., The formation of trace element-enriched particulates during laser ablation of refractory materials. *Spectrochimica Acta Part B* **1996**, 51, 1451-1462.
50. Čtvrtníčková, T.; Fortes, F. J.; Cabalin, L. M.; Laserna, J. J., Optical restriction of plasma emission light for nanometric sampling depth and depth profiling of multilayered metal samples. *Applied Spectroscopy* **2007**, 61, (7), 719-724.
51. Silverstein, R. M.; Webster, F. X.; Kiemle, D. J., *Spectrometric Identification of Organic Compounds*. 7th ed.; John Wiley & Sons, Inc.: Hoboken, NJ, 2005; p 502.
52. Reffner, J. A.; Martoglio, P. A., Uniting Microscopy and Spectroscopy. In *Practical Guide to Infrared Microspectroscopy*, Humecki, H. J., Ed. Marcel Dekker, Inc.: New York, 1995; Vol. 19.
53. Skoog, D. A.; Holler, F. J.; Crouch, S. R., *Principles of Instrumental Analysis*. Brooks Cole: 1997.
54. Goldstein, J. I.; Newbury, D. E.; Echlin, P.; Joy, D. C.; Romig, A. D.; Lyman, C. E.; Fiori, C.; Lifshin, E., *Scanning electron microscopy and X-ray microanalysis: a text for biologists, materials scientists, and geologists*. 2nd ed.; Plenum Press: New York, 1992; p 820.
55. Coombes, K. R.; Fritsche Jr., H. A.; Clarke, C.; Chen, J.-N.; Baggerly, K. A.; Morris, J. S.; Xiao, L.-C.; Hung, M.-C.; Kuerer, H. M., Quality control and peak finding for proteomics data collected from nipple aspirate fluid by surface-enhanced laser desorption and ionization. *Clinical Chemistry* **2003**, 49, (10), 1615-1623.
56. Scientific, T. Spectral Library Search, Correlation Algorithm. [http://www.thermo.com/com/cda/resources/resources\\_detail/1,,13437,00.html](http://www.thermo.com/com/cda/resources/resources_detail/1,,13437,00.html)
57. O'Rourke, N.; Hatcher, L.; Stepanski, E. J., *A step-by-step approach to using SAS® for univariate & multivariate statistics*. 2nd ed.; SAS Institute and John Wiley & Sons, Inc.: Cary, NC, 2005.
58. Johnson, S. C., Hierarchical clustering schemes. *Psychometrika* **1967**, 32, 241-245.
59. Sigman, M. E.; Williams, M. R.; Ivy, R. G., Individualization of Gasoline Samples by Covariance Mapping and Gas Chromatography/Mass Spectrometry. *Analytical Chemistry* **2007**.
60. Eiler, A.; Bertilsson, S., Composition of freshwater bacterial communities associated with cyanobacterial blooms in four Swedish lakes. *Environmental Microbiology* **2004**, 6, (12), 1228-1243.

61. Gribskov, M.; Robinson, N. L., Use of receiver operating characteristic (ROC) analysis to evaluate sequence matching. *Computers and Chemistry (Oxford)* **1996**, 20, (1), 25-33.
62. Limpert, E.; Stahel, W. A.; Abbt, M., Log-normal distributions across the sciences: keys and clues. *BioScience* **2001**, 51, (5), 341-352.
63. Lentjes, M.; Dickmann, K.; Meijer, J., Calculation and optimization of sample identification by laser induced breakdown spectroscopy via correlation analysis. *Spectrochimica Acta Part B* **2007**, 62B, (1), 56-62.
64. Michel, A. P. M.; Chave, A. D., Analysis of laser-induced breakdown spectroscopy spectra: The case for extreme value statistics. *Spectrochimica Acta Part B* **2007**, 62B, (12), 1370-1378.
65. Hotelling, H., New light on the correlation coefficient and its transforms. *Journal of the Royal Statistical Society B* **1953**, 15, (2), 193-225.
66. Harrison, G. R., *Massachusetts Institute of Technology Wavelength Tables*. Halliday Lithograph Corporation: Cambridge, MA, 1991.
67. Ryland, S. G., Infrared Microspectroscopy of Forensic Paint Evidence. In *Practical Guide to Infrared Microspectroscopy*, Humecki, H. J., Ed. Marcel Dekker, Inc.: New York, 1995; Vol. 19, pp 163-244.
68. Cravetchi, I. V.; Taschuk, M. T.; Tsui, Y. Y.; Fedosejevs, R., Evaluation of femtosecond LIBS for spectrochemical microanalysis of aluminium alloys. *Analytical and Bioanalytical Chemistry* **2006**, 385, 287-294.
69. Gornushkin, I. B.; Smith, B. W.; Nasajpour, H.; Winefordner, J. D., Identification of solid materials by correlation analysis using a microscopic laser-induced plasma spectrometer. *Analytical Chemistry* **1999**, 71, (22), 5157-5164.
70. Thornton, J. I., The General Assumptions and Rationale of Forensic Identification. In *Modern Scientific Evidence: The Law and Science of Expert Testimony*, Faigman, D. L.; Kaye, D. H.; Saks, M. J.; Sanders, J., Eds. West Publishing Co.: 1997; Vol. 2.
71. De Lucia Jr., F. C.; Gottfried, J. L.; Munson, C. A.; Miziolek, A. W., Double pulse laser-induced breakdown spectroscopy of explosives: Initial study towards improved discrimination. *Spectrochimica Acta Part B* **2007**, 62B, (12), 1399-1404.
72. Maritz, J. S., *Distribution-free statistical methods*. 2nd ed.; Chapman & Hall: New York, 1995; p 255.
73. Sprent, P.; Smeeton, N. C., *Applied nonparametric statistical methods*. 3rd ed.; Chapman & Hall: Boca Raton, FL, 2001; p 461.



74. Dudley, R. J.; Smalldon, K. W., The Comparison of Distributional Shapes with Particular Reference to a Problem in Forensic Science. *International Statistical Review / Revue Internationale de Statistique* **1978**, 46, (1), 53-63.